International Atomic Energy Agency

INDC(GDR)-057
Distr.: L

INDC INTERNATIONAL NUCLEAR DATA COMMITTEE

CONTRIBUTIONS TO THE THEORY OF FISSION NEUTRON EMISSION

D. Seeliger, H. Märten and A. Ruben
Technische Universität Dresden
Mommsenstrasse 13, DDR-8027 Dresden, German Democratic Republic

March 1990

INDC(GDR)-057
Distr.: L

CONTRIBUTIONS TO THE THEORY OF FISSION NEUTRON EMISSION

D. Seeliger, H. Märten and A. Ruben
Technische Universität Dresden
Mommsenstrasse 13, DDR-8027 Dresden, German Democratic Republic

March 1990

Abstract

This report gives a compilation of recent work performed at Technical University, Dresden by D. Seeliger, H. Märten and A. Ruben on the topic of fission neutron emission. In the first paper calculated fission neutron spectra are presented using the temperature distribution model FINESSE for fissioning actinide nuclei. In the second paper, starting from a general energy balance, Terrell's approach is generalized to describe average fragment energies as a function of incident energy; trends of fragment energy data in the Th-Pu region are well reproduced. In the third contribution, prompt fission neutron spectra and fragment characteristics for spontaneous fission of even Pu-isotopes are presented and discussed in comparison with experimental data using a phenomenological scission point model including temperature dependent shell effects. In the fourth paper, neutron multiplicities and energy spectra as well as average fragment energies for incident energies from threshold to 20 MeV (including multiple-chance fission) for U-238 are compared with traditional data representations.

Reproduced by the IAEA in Austria
March 1990

90-00861

Contents

FISSION NEUTRON STATISTICAL EMISSION

A. Ruben, H. Märten, and D.Seeliger
Technische Universität Dresden
Mommsenstr.13, DDR-8027, German Democratic Republic

Abstract - *The statistical model approach FINESSE (FIssion NEutronS' Statistical Emission) for the description of fission neutron multiplicities, energy spectra and angular distributions is described . Based on an extended Weisskopf ansatz and on a realistic temperature distribution it provides a fragment mass number dependent description of fission neutron data. Model parameters (optical potential, n/γ competition) were fixed on the basis of the ^{252}Cf(sf) (nuclear data standard). Combined with a phenomenological fission model for predicting relevant fragment data as function of asymmetry, FINESSE can be applied to any fission reaction of actinides in the Th-Cf region without further parameter adjustment. Results are presented for ^{252}Cf(sf) and neutron induced fission of ^{235}U, ^{239}Pu, ^{232}Th. Effects of multiple-chance fission are discussed for ^{232}Th(n,xnf) reaction.*

I. INTRODUCTION

For many applied purposes in different fields as fission technology, nuclear safeguards, and nuclear power engineering the exact knowledge of fission neutron data is required. In general, these spectra are described by either a Maxwellian

$$N(E) = \bar{\nu} \frac{2}{\sqrt{\pi} T_M^{3/2}} \sqrt{E} \exp\left[-\frac{E}{T_M}\right] \qquad (1)$$

(E - neutron energy, T_M - Maxwellian temperature) or a Watt[1] distribution involving one or two free parameters, respectively. However, both ansatzes are only rough approximations, whose parameters have been empirically deduced for applications.

Due to the complexity of the fission process and the corresponding influence on prompt fission neutron emission, the determination of more realistic spectra should be based on an adequate statistical model approach (SMA) in conjunction with fission theory to deduce the intricate fragment distribution[2].

As found in several recent works[3-6], fission neutrons are mainly released due to evaporation from fully accelerated fragments. Emission processes close to scission point (scission neutrons; neutrons emitted during fragment acceleration[7]) are secondary (yield < 5 %[5,6]).

Consequently, the SMA can be based on an "asymptotic" fragment distribution (i.e. after fragment acceleration and dissipation of fragment excitation energy) and the assumption of statistical emission from equilibrated, highly excited fragments.

A general theoretical concept for the description of prompt fission neutron emission as a fragment de-excitation process as well as different models were presented in ref.[2,5]

Following the general concept, these SMA differ in regard of two main items:

(i) spectrum ansatz in the center-of-mass system (CMS) (Hauser-Feshbach theory[8], Weiskopf-Ewing ansatz[9], statistical multistep compound theory[5] or any approximative spectrum);

(ii) degree of consideration of the complex fragment occurrence probability P(A,Z,TKE,E*,I...) as a function of the fragment characteristics mass, charge, total kinetic energy, excitation energy, angular momentum, respectively.

A more detailed analysis of fission neutron spectra, e.g. the consideration of all important fragment distributions, requires the exact knowledge of these distribution functions (at least for asymptotic conditions discussed above). Sufficient experimental data exist only for a few fission reactions (e.g. ^{252}Cf(sf), ^{235}U(n_{th},f)).

In order to do systematic calculations of prompt fission neutron data on the basis of a tractable model, a simplified SMA is required, for which all necessary input data are available. For applied purposes Madland and Nix[10] proposed a temperature-distribution model (Madland-Nix model MNM) including a spectrum description for the most probable fragment pair. This approach has been generalized in Ref.[11] in order to incorporate the full dependence of spectral shape on fragment mass number (Generalized Madland-Nix model GMNM). The present work relies on basic ideas of the GMNM. However essential changes concern

- CMS spectrum ansatz including anisotropy due to fragment spin,
- temperature distribution,
- consideration of n/γ competition of fragment de-excitation,
- range of applicability, e.g. multiple chance fission.

This new SMA called FINESSE (code name) as well as several applications are described in detail in this work.

II. THE MODEL

A) CMS SPECTRUM ANSATZ

Evaporation of neutrons from fully accelerated fragments is assumed as the main neutron emission mechanism. According to the statistical nuclear theory[5] the evaporation spectrum $\varphi(\varepsilon:A)$ for given mass number A and excitation energy E^* is described by

$$\varphi(\varepsilon:A) \simeq \varepsilon\, \sigma(\varepsilon:A)\, \rho(U:A) \qquad (2)$$

(ε - CMS neutron energy, $\sigma(\varepsilon:A)$ - cross section) including the level density ρ as a function of rest-nucleus excitation energy U, i.e.

$$U = E^* - \varepsilon - B_n \qquad (3)$$

(E^* - excitation energy of fragment before neutron emission, B_n - neutron binding energy). Taylor expansion of entropy S (following from level density $S=\int dE/T=\ln(\rho)$) by using the thermodynamical relation between U and temperature t

$$U = a(A)\, t^2 \qquad (4)$$

(a - level density parameter) results in a first order to the well known Weisskopf equation[5]. Considering the second term of expansion, too, one gets

$$\varphi(\varepsilon:A) \simeq \varepsilon\, \sigma(\varepsilon:A)\, \exp\left\{-\frac{\varepsilon}{T} - \frac{\varepsilon^2}{4a(A)T^3}\right\} \qquad (5)$$

T is the maximum rest nucleus temperature, i.e. for $\varepsilon = 0$. According to Eq. (3) it is related to $U_{max} = E^* - B_n$. In contrast to the Weisskopf equation[5] this evaporation ansatz includes the cooling of the rest-nucleus due to neutron evaporation, which has an influence especially on the high-energy part of the spectrum ($\varepsilon > \bar{\varepsilon}$). The cross-section σ can be assumed to be equal to that of the inverse reaction, i.e. the formation of compound nucleus by absorption of a neutron. These data depending on neutron energy ε and fragment mass A are obtained in the framework of optical model calculations based on a global optical potential. It will be discussed in paragraph IV.A.

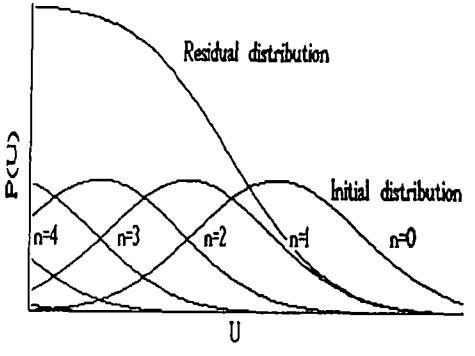

Fig. 1 Distribution in residual nucleus excitation energy U assumed as sum of all excitation energy distributions of cascade emission steps n≥1. The initial distribution (n=0) is also shown.

The initial distribution in excitation energy of a fragment as well as cascade emission are considered by assuming a distribution in residual nucleus temperature P(T:A) corresponding to a distribution in E^* for all cascade emission steps ≥ 1

$$P(U:A) = \sum_{i\geq 1} P_i(E^*:A) \cong \frac{1}{1 + \exp\left[\frac{U - \hat{U}(A)}{d(A)}\right]} \qquad (6)$$

As illustrated in Fig.1, the "edge parameter" $\hat{U}(A)$ is equal to the half distance between average initial excitation energy and that after first neutron emission. It can be well approximated by

$$\hat{U}(A) = \bar{E}^*(A) - \tfrac{1}{2}\, \bar{B}_n(A)\ . \qquad (7)$$

Note that all plotted curves in Fig. 1 show distributions in maximum rest-nucleus excitation energy ($\bar{\varepsilon} = 0$). The second parameter d(A) denotes the "diffuseness" of an approximative dependence of the variance of the initial distribution, $P_0(E^*,A)$

on average initial excitation energy[12], i.e.

$$\sigma_E^2 (A) \approx 3.3 \text{ MeV } \overline{E^*}(A). \qquad (8)$$

Based on this empirical relation one gets

$$d(A) \approx \frac{1}{5} \overline{E^*}(A). \qquad (9)$$

Using the Fermi-gas model equation (4) P(U:A) is transformed into the temperature distribution needed

$$P(T:A)dT = \frac{\partial U}{\partial T} P(U:A)dT = \frac{2\, a(A)\, T}{1+ \exp\left[\frac{a(A)T^2 - \hat{U}(A)}{d(A)}\right]} dT \qquad (10)$$

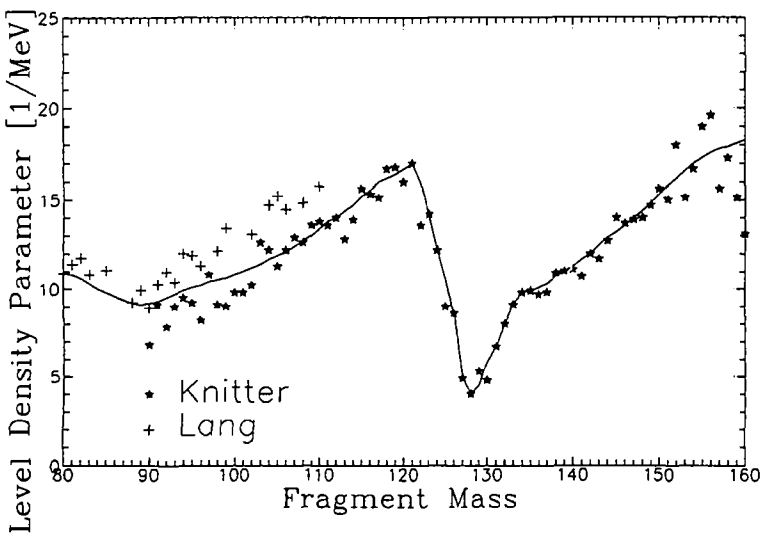

Fig. 2 Effective values of the level density parameter as function of fragment mass number. Experimental data were taken from Refs.[6,13]. The solid line represents a spline fitted curve used within FINESSE.

The level density parameter a(A) entering this equation is taken from the results of Knitter (^{252}Cf(sf))[6] added by data of Lang [18] for very light fragments (^{235}U(n_{th},f)). In order to apply these data for a wide range of fissioning nuclei they where smoothed as shown in Fig.2. These a(A) values are assumed to be representative for fission fragments with typical excitation energies between 5 and 30 MeV.

Following the presented formalism the CMS-neutron spectrum for a fragment with mass number A is given by

$$\varphi(\varepsilon:A) = \sigma_{inv}(\varepsilon:A)\, \varepsilon \int_{T_o}^{\infty} K(T:A)\, P(T:A) \exp\left\{-\frac{\varepsilon}{T} - \frac{\varepsilon^2}{4a(A)T^3}\right\} dT. \qquad (11)$$

K(T:A) is a temperature-dependent normalization constant

$$K(T:A) = \left[\int_0^{\infty} \sigma_{inv}(\varepsilon:A)\, \varepsilon \exp\left\{-\frac{\varepsilon}{T} - \frac{\varepsilon^2}{4a(A)T^3}\right\} d\varepsilon\right]^{-1}. \qquad (12)$$

To consider neutron-γ competition of fragment de-excitation the lower integration limit T_o is introduced. Up to T_o only γ-ray emission is assumed. This is confirmed by the fact that γ-emission appears especially for excitation energies just above neutron binding energy reducing P(T) at very low temperature. This value is used as a free parameter for model adjustment (see paragraph 4.1).

B) CMS ANISOTROPY

In order to account for CMS anisotropy[14,15] of prompt fission neutrons the CMS-spectrum (Eq. 10) is generalized by a correction function

$$\varphi(\varepsilon,\vartheta:A) = \varphi(\varepsilon:A)\, F(\vartheta) \qquad (13)$$

ϑ is the CMS angle of neutron emission with reference to fragment direction. Based on the semi-classical treatment of Ericson and Strutinski[16] the spin-dependent neutron CMS anisotropy has been estimated. In agreement with Gavron[17] we assume

$$F(\vartheta) = \frac{1}{4\pi} \frac{1 + \beta \cos^2\vartheta}{1 + \beta/3} \qquad (14)$$

with the anisotropy parameter $\beta \approx 0.1$. Actually, β depends on ε[16]. However, a linear dependence as consequence of the distribution given in Ref.[16] seems to be too strong (cf. Ref.[14]). Actually, the influence of fragment spin on spectrum shape has to be described in the framework of Hauser-Feshbach theory[8] as done in Ref.[17] for ^{252}Cf(sf).

C) CMS-LS-TRANSFORMATION

The calculated single-fragment CMS neutron distributions have to be transformed into the laboratory system resulting in $N(E,\theta:\delta\alpha)$. E and $\tilde{\theta}$ are the LS coordinates. The angle $\tilde{\theta}$ is defined with reference to fragment direction. Due to the different fragment velocities (given by kinetic energy and by mass) this CMS-LS transformation has to be done before summing up the distributions from different fragments weighted by their yield. Momentum conservation results in the kinematical relations

$$E = E_f + \varepsilon + 2\sqrt{E_f\,\varepsilon}\,\cos\vartheta, \tag{15}$$

$$\varepsilon = E + E_f - 2\sqrt{E\,E_f}\,\cos\tilde{\theta} \tag{16}$$

with the kinetic energy per nucleon E_f of the fragment

$$E_f = \overline{TKE}(A_1,A_2)\left[\frac{1}{A} - \frac{1}{A_{FN}}\right] \tag{17}$$

(A_{FN}- mass number of fissioning nucleus). Emission probability transformation from CMS into LS results in

$$N(E,\tilde{\theta}:\alpha) = \sqrt{\frac{E}{\varepsilon}}\;\varphi(\varepsilon,\vartheta:A) \tag{18}$$

The final LS distribution is given by the superposition of all fragment spectra weighted by the mass yield Y(A)

$$N(E,\theta) = \sum_A N(E,\tilde{\theta}:A)\;Y(A)\;\bar{\nu}(A), \tag{19}$$

where $\tilde{\theta} = \begin{cases} \theta & \text{for light fragments} \\ \pi-\theta & \text{for heavy fragments} \end{cases}$.

Here, θ is the LS angle of neutron emission with reference to light-fragment direction.

D) MASS YIELD

The involved fragment mass distribution Y(A) is obtained by superposition of 5 Gaussians, which are characterized by average value, variance and weight. These parameters depend on mass and excitation energy of the fissioning nucleus and have been fitted on the basis of experimental data for the Th-Cf region. In special cases it is proper to consider original experimental data on Y(A) for calculations concerning Eq. (18). The 5-Gaussian approximation involving two asymmetric and one symmetric component corresponds to fission modes which are predominant in the case of actinide fission.

E) NEUTRON MULTIPLICITY

The final distribution is normalized to the total average neutron multiplicity $\bar{\nu}_{tot}$. This is done on the basis of the fragment neutron multiplicities deduced in an energy balance of fragment de-excitation including evaporation of neutrons (multiplicity $\bar{\nu}$, average CMS energy $\bar{\varepsilon}$) and γ-ray emission (average total energy $\bar{E}_\gamma$),

$$\bar{E}^*(A_i) = \bar{\nu}(A_i)\,(\bar{B}_n(A_i) + \bar{\varepsilon}(A_i)) + \bar{E}_\gamma(A_i). \tag{20}$$

The neutron separation energy $\bar{B}_n(A)$ is calculated on the basis of mass tables[18] using an approximated charge distribution according to Wahl[19] and considering the increase of $\bar{B}_n(A)$ with $\bar{\nu}$. This is due to the shift of the fission fragments towards the line of β-stability and is approximated by

$$\bar{B}_n(A) = \bar{B}_n^{z-dis}(A) + C\;\bar{\nu}(A) \tag{21}$$

with the correction factor $C \cong 0.1$ for U isotopes, $\cong 0.3$ for Cf. According to the results of Frehaut[20] the average total gamma energy is assumed to be linear in neutron multiplicity. Thus, $\bar{E}_\gamma(A_i)$ is given in the Th-Cf region by the following approximation,

$$\bar{E}_\gamma(A) = [\,G_1\;\bar{\nu}(A) + 2.2\,]\ \text{MeV}. \tag{22}$$

The constant G_1, which depends on the mass of the fissioning nucleus is taken from Frehaut[20]

F) ENERGY PARTITION IN FISSION

The average excitation energy $\bar{E}^*(A)$ as well as the total kinetic energy as function of mass split $\overline{TKE}(A_1/A_2)$ are obtained in the framework of a phenomenological scission point model including semi-empirical, temperature-dependent shell correction energies

for deformed fragments at scission (two-spheroid model TSM[21]). This model involves a general energy balance of the fissioning nucleus at scission with respect to saddle point conditions. It is applicable to any induced fission reaction with actinides. As shown in Ref.[21], TSM reproduces striking trends of mass-asymmetry dependent fragment energies as function of incidence energy.

Based on TSM as well as the 5-Gaussian description of mass yield, the SMA concept outlined above can be used to predict double-differential emission probabilities as well as angular integrated distributions (energy spectra N(E)).

G) DOUBLE-DIFFERENTIAL EMISSION CROSS SECTION IN INDUCED FISSION

In the case of induced fission reactions, it is appropriate to describe the emission probability with reference to the incidence particle direction. This distribution $G(E,\psi)$ (ψ-neutron emission angle with reference to incidence direction) can be obtained by folding up $N(E,\theta)$ with the fragment angular distribution $W(\alpha)$. By the help of a Legendre polynom expansion of both $N(E,\theta)$ and $W(\alpha)$, the folding integral is given by the simple equation

$$G(E,\psi) = \sum_n A_n B_n \frac{2}{2n+1} P_n(\cos\psi) \qquad (23)$$

with the Legendre polynoms B_n for the fragment angular distribution (measured data)

$$W(\alpha) = \sum_n B_n P_n(\cos\alpha) \qquad (24)$$

and the polynoms $A_n(E)$ fitted from the neutron distribution (θ' with reference to fission axis) according to[22,23]

$$N'(E,\theta') = \frac{1}{2}\left(N(E,\theta) + N(E,\Pi-\theta)\right) = \sum_n A_n P_n(\cos\theta'). \qquad (25)$$

In this equation, N' is a symmetric (with reference to $\theta'=90°$) distribution. Within FINESSE, the total LS distribution $N'(E,\theta')$ is transformed into $G(E,\psi)$ neglecting the mass number dependence of fragment angular distribution $W(\alpha)$. However, this dependence has a minor influence on the transformation. Therefore, the approximation according to Eqs.(23-25) is justified.

Multiplying the emission probability $G(E,\psi)$, which is normalized to $\bar{\nu}_{tot}$, by the fission cross section σ_f the double-differential emission cross section of fission neutrons is obtained.

H) MULTIPLE-CHANCE FISSION

In the case of high incidence energies ($\geq$ 6 MeV for neutrons) multiple chance reactions appear, e.g. (n,xnf) for neutron induced fission. Because of considerable differences of fragment distributions corresponding to the chances at one given incidence energy, the neutron distributions $G(E,\psi)$ are calculated separately. The partial fission cross section $\sigma_{f,x}$ for chance x (x=0,1,2,...) corresponds to its weight. Consequently, the total emission probability is given by

$$G_{tot}(E,\psi) = \frac{1}{\sigma_f} \sum_{x=0}^{x^{max}} G_x(E,\psi)\ \sigma_{f,x} \qquad (26)$$

where

$$\sigma_f = \sum_{x=0}^{x^{max}} \sigma_{f,x} \qquad (27)$$

$G_{tot}(E,\psi)\ \sigma_f$ is the double-differential emission cross section of post-fission neutrons (cf. II.G).

The partial fission cross sections $\sigma_{f,x}$ have to be calculated in the framework of reaction theory including the fission channel. Possible methods are the use of Hauser-Feshbach theory[8] extended by pre-equilibrium contributions as available with the code STAPRE[24,25] or the treatment proposed by Madland and Nix[10].

Obviously, the excitation energy of fissioning nuclei corresponding to higher-order chances ($x \geq 1$) is distributed according to the emission spectra of pre-fission neutrons. In most cases, it is justified to calculate the post-fission neutron emission probability $G_x(E,\psi)$ for $x \geq 1$ on the basis of an average excitation energy of the fissioning nuclei, i.e. the TSM and the 5-Gaussian approach to the mass yield are applied only once for a chance $x \geq 1$. This approximation doesn't yield any remarkable differences from the exact calculation. Deviations are within the general theoretical uncertainty. On the other hand, the approach described is not as time-consuming as calculations including the full dependence on fissioning-nucleus excitation energy for higher-order chances.

III. RESULTS

A) THE ^{252}Cf(sf) NEUTRON SPECTRUM

As a relative well-known distribution the standard energy spectrum of prompt neutrons from spontaneous fission of ^{252}Cf was taken to adjust the only free parameter T_o of FINESSE. Criterion for this adjustment was the agreement of the calculation with the average LS-neutron energy $\bar{E}$, which has been obtained by direct integration. Based on the evaluation of Mannhart[26] one gets T_o = 0,22 - 0,36 MeV depending on the optical potential[27-30] considered in calculation of inverse cross section $\sigma_{inv}(\epsilon:A)$. As plotted in Fig.3, these differences in σ_{inv} give rise to remarkable changes,

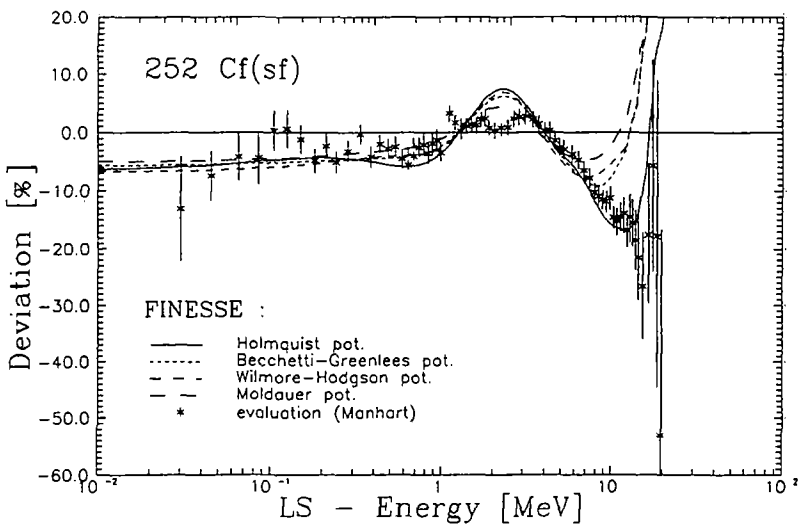

Fig. 3 Calculated prompt fission neutron spectrum for ^{252}Cf(sf) represented as deviation from a Maxwellian with T_M = 1.42 MeV in comparison with the evaluation of Mannhart[26]. Calculations were based on several optical potentials as indicated (Refs.[27-30]).

especially in the high-energy region of the neutron spectrum. It has to be pointed out that these changes as well as the shape of the prompt fission neutron spectrum itself is very similar to the results of calculations in the framework the cascade-evaporation model[12,31] (CEM). Note that the spectrum tail at energies above ≅ 15 MeV is very sensitive with respect to changes in the fragment distribution.[32]

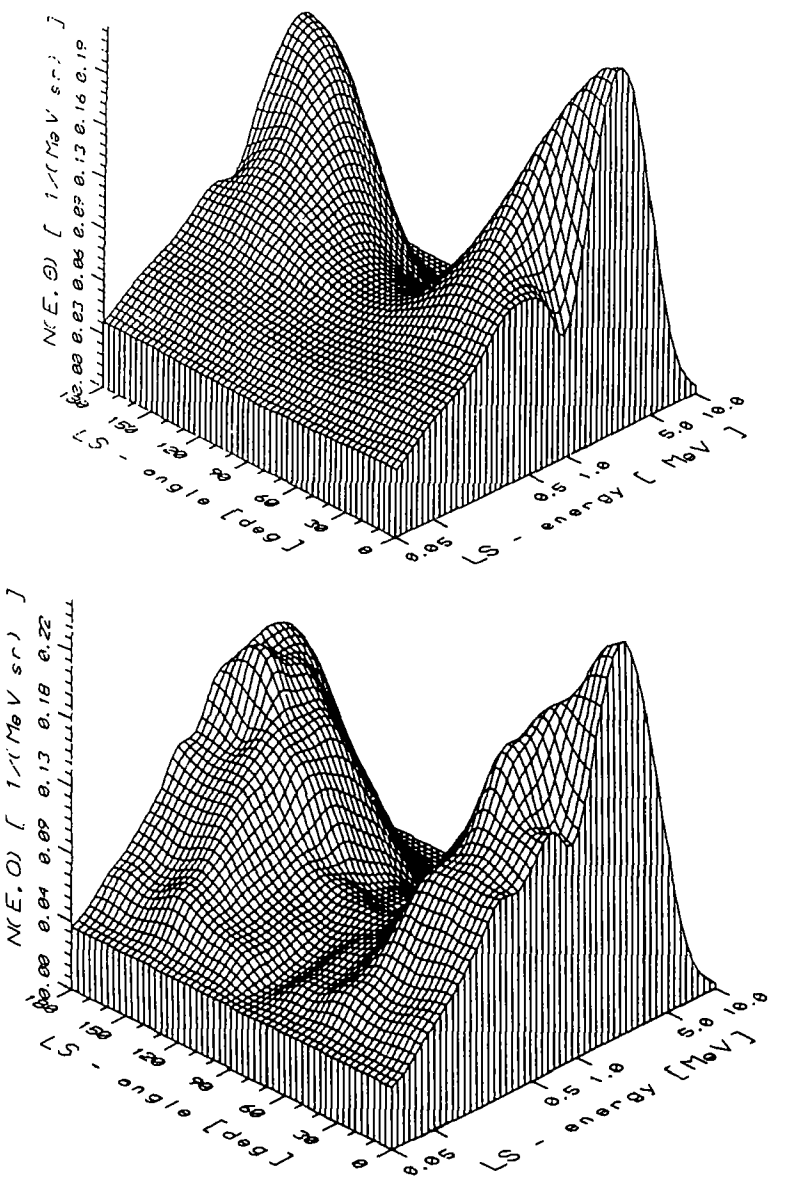

Fig. 4 Angular and energy distribution of emitted prompt fission neutrons in the laboratory system for ^{252}Cf(sf) (top-calculation, bottom-experimental data taken from Ref.[33]).

In addition to the comparison of calculated spectra with the evaluation, double-differential emission probabilities $N(E,\theta)$ have been considered. The best description of the integral spectrum as well as of the angular distributions has been obtained using the Holmqvist[30] potential. Fig.4 shows the double differential emission probability $N(E,\theta)$ in comparison with measured data[39]. Note that the general behaviour of this distribution as the remarkable structure in the 0° and 180° region at E close to 0.98 MeV and 0.55 MeV, respectively, due to kinematical effects (low-energy neutron emission in CMS) is well reproduced by the FINESSE calculation. Hence, the conclusion can be drawn that the assumed emission mechanism is the predominant one.

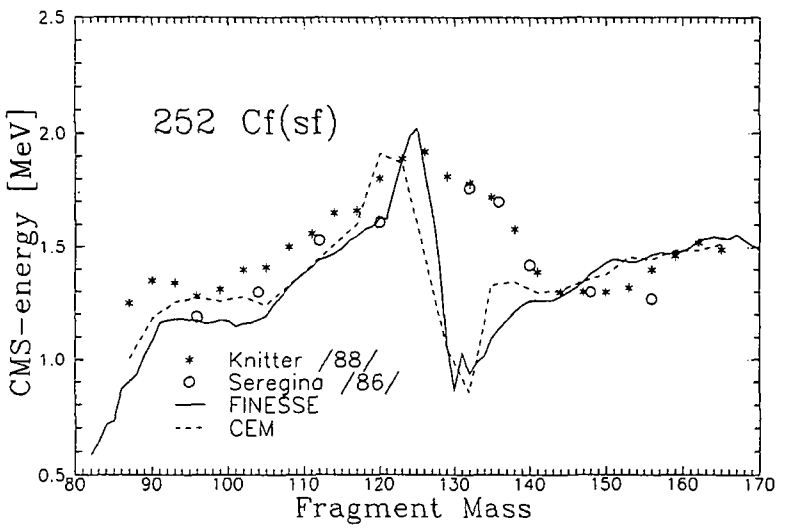

Fig. 5 Average CMS neutron energy as function of fragment mass number for $^{252}Cf(sf)$ (solid line - FINESSE calculation, dashed line - cascade evaporation model[12,31], points - experimental data taken from Refs.[4,6]).

Fig.5 shows the average neutron energy in the CMS depending on fragment mass number. The calculated values (FINESSE and CEM) are compared with experimental data deduced by Knitter and Budtz-Jorgensen[6] and Seregina et al.[4] Excepting the heavy-fragment region with mass number close to 130, the calculated and measured data are in a good agreement. At A ≅ 130, the influence of secondary fission modes[17] with large heavy-fragment deformation,

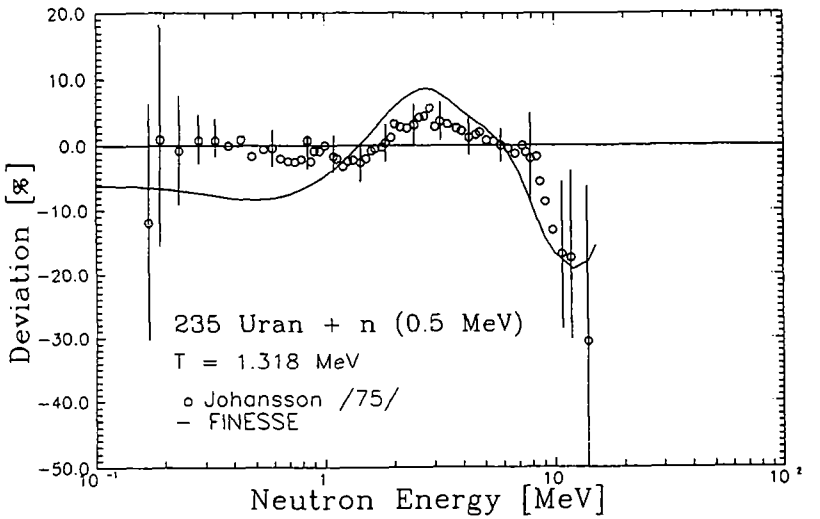

Fig. 6 Calculated prompt fission neutron spectrum for $^{235}U(n,f)$ at 0.5 MeV incidence energy plotted as deviation from a Maxwellian with T_M = 1.318 MeV in comparison with experimental data[34].

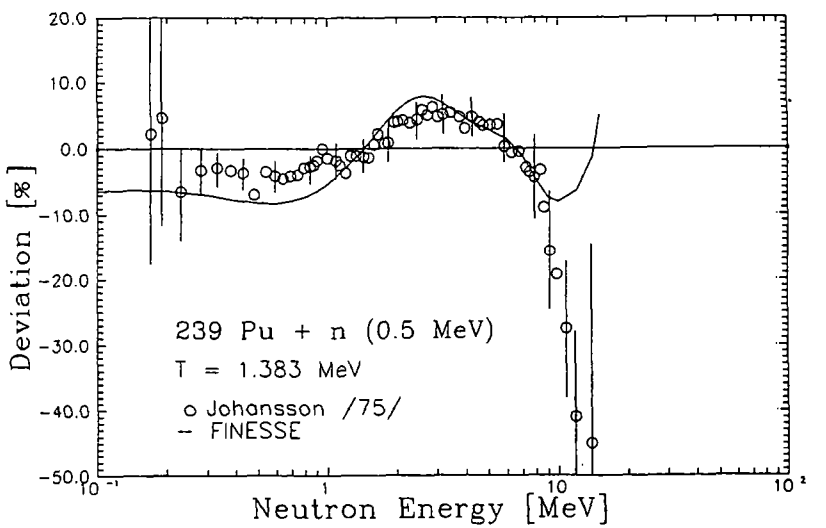

Fig. 7 As for Fig. 6, but for $^{239}Pu(n,f)$ with reference to a Maxwellian with T_M = 1.383 MeV (experimental data taken from Ref.[34]).

i.e. high fragment excitation energy, leads to rather high average CMS neutron energy, whereas the less-deformed double-magic fragments belonging to the predominant fission mode (for the given mass split) do not emit neutrons due to the very low excitation energy. Consequently, in spite of the low total neutron multiplicity for A ≅ 130, the average CMS energy is rather high. However, this mass number region corresponds to a small fragment yield. Therefore, the effect discussed has no considerable influence on the total neutron emission probability. FINESSE reproduces the Cf standard neutron spectrum in a wide energy range. As already discussed in Ref.[14], the consideration of CMS anisotropy of neutron emission results in a more reliable description of the total energy spectrum at low energy. Here, the optical potential and the fragment energies have less influence.

B) ENERGY DEPENDENCE OF INDUCED-FISSION NEUTRON SPECTRA

Considering the Holmqvist potential as well as the T_0 value adjusted on the basis of the Cf standard spectrum, FINESSE combined with TSM and 5-Gaussian approach to fragment mass yield can be applied to any fission reaction without any parameter changes.

The incidence energy dependence of neutron emission spectra has been studied in the case of the neutron induced fission of ^{235}U and ^{239}Pu. Experimental data exist only for a few incidence energies points. In contrast to the $^{252}Cf(sf)$-standard spectrum, the shape of those fission neutron spectra is less certain in most cases. Further, the energy range covered in the experiments is often limited due to special conditions in the experiments (background, detector type). As well established examples, we consider the fission neutron spectra measured by Johansson et al.[34] Figs. 6 and 7 represent the deviation of neutron spectra from a Maxwellian (Eq. 1) for the 0.5 MeV neutron induced fission of ^{235}U and ^{239}Pu, respectively. The data are well reproduced by TSM-FINESSE. Note that the average energies of the calculated neutron spectra (and, consequently, Maxwellian temperature T_M) are about 2% higher then those deduced by Johansson et al. The slight overestimation of the experimental spectra by the calculation between 4 and 7 MeV points to a somewhat higher Maxwellian temperature compared to the value given by Johansson et al.

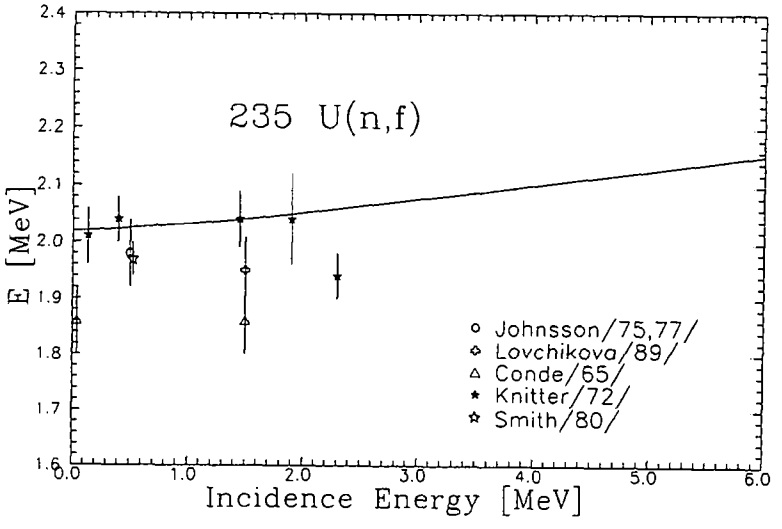

Fig. 8 Average LS neutron energy as function of incidence energy for $^{235}U(n,f)$ (solid line - FINESSE calculation, experimental data - Ref.[34-39]).

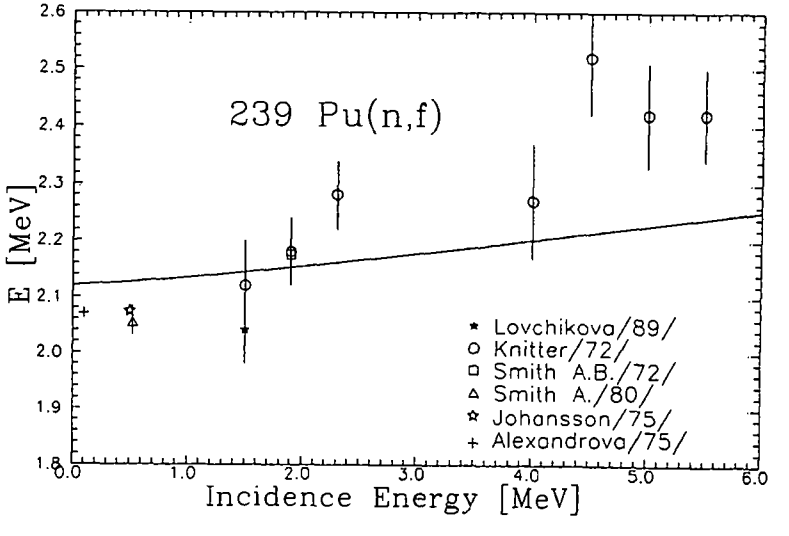

Fig. 9 Average energy of the LS neutron spectrum as function of incidence energy for $^{239}Pu(n,f)$ (solid line - FINESSE calculation, experimental data - Ref.[34-36,38,40,41]).

For systematic studies the most important quantity is the average energy $\bar{E} = 1.5\ T_M$ of the emitted neutrons. In Fig. 8 and 9 the dependence of $\bar{E}$ on the incidence energy is shown for the two fissioning nuclei. The calculated data differ from the experimental ones up to 10%. It has to be emphasized that a fit of experimental data to a Maxwellian distribution is influenced by the energy range considered. One should account for deduced T_M as effective values. Due to the typical spectral shape as shown in Figs. 3, 5, and 6, fitted T_M values differ remarkably, if considering only the low-energy ($\leq$ 2 MeV) or the high-energy ($\geq$ 2 MeV) part. In particular, the neglect of the low-energy region part leads to an underestimation of $\bar{E}$. Therefore, only a qualitative comparison between experimental and theoretical values is possible. As depicted in the figures, the general increase of the average neutron energy with incidence energy is well reproduced.

As shown in paragraph III.A. for the spontaneous fission of ^{252}Cf (cf. Fig. 4) it is possible to calculate both energy and angular distributions of prompt fission neutrons. For induced fission reactions the angular distribution in the laboratory system with reference to the direction of the incidence particle is of interest. Thus, the fragment angular distribution has to be taken into account according to Eq. (20). The neutron anisotropy with reference to incidence-beam direction increase with neutron energy. This increase depends on incidence energy. To illustrate this behaviour, Fig. 10 shows the asymmetry (0°/90°-ratio) of the neutron spectrum for the neutron induced fission of ^{238}U at different incidence energies. In general, a higher neutron anisotropy is found in the case of threshold fission (1.5 MeV) due to the large fragment anisotropy. For higher incidence energies the decreasing fragment anisotropy leads to lower 0°/90°-neutron ratio.

C) NEUTRON SPECTRA FOR MULTIPLE CHANCE FISSION

In the case of high incidence energy ($E_i > B_i$, B_i- binding energy of incidence particle) neutron emission prior to fission becomes energetically possible. Consequently, different fission chances (n,xnf) with x=0,1,2,... occur. The calculation of the prompt fission neutron spectra in the case of these so-called multiple chance fission reactions have been explained in paragraph II.H. As

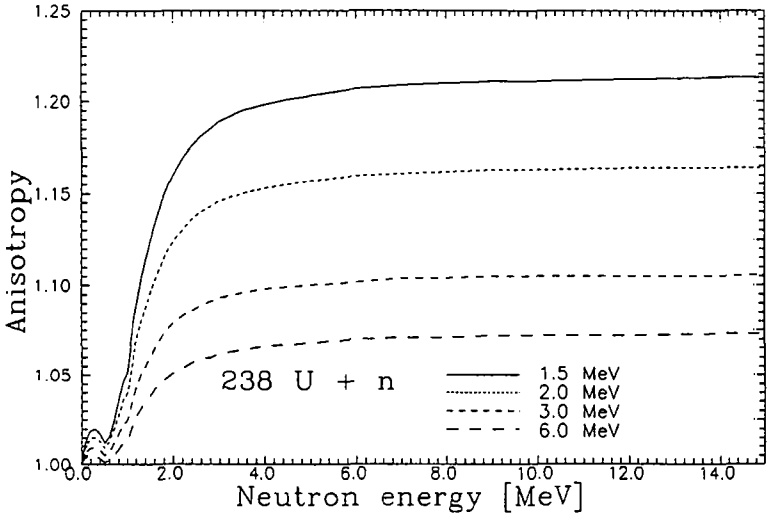

Fig. 10 LS-anisotropy (0°/90°-ratio) of emitted neutrons as function of neutron energy plotted for different incidence energies of $^{238}U(n,f)$ (fragment anisotropy taken from Ref.[46]).

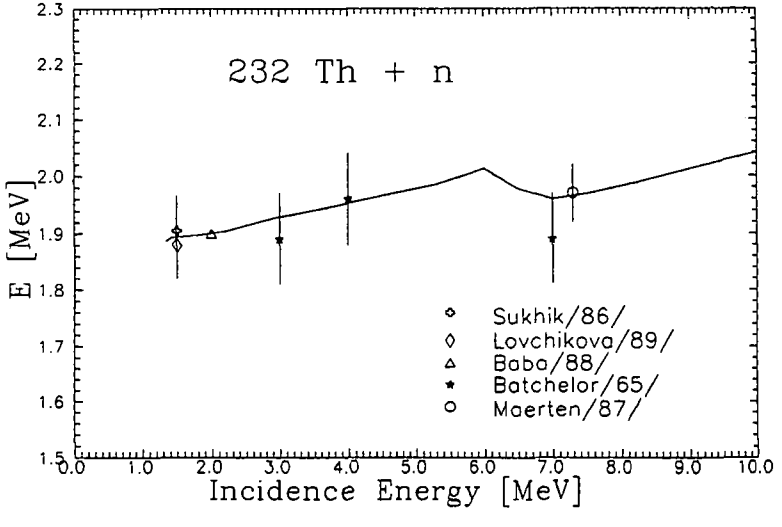

Fig. 11 Average energy of the LS-neutron spectrum as function of incidence energy for neutron induced fission of ^{232}Th (solid line - FINESSE calculation, experimental data were taken from Ref.[36,42-44]).

an example, the emission spectra for the neutron induced fission of ^{232}Th have been calculated up to 10 MeV incidence energy. In Fig. 11, the calculated average neutron energies are presented as function of incidence energy. In the case of multiple chance fission, $\bar{E}$ is deduced by superposition of those values $\bar{E}_x$ of the several chances x according to,

$$\bar{E} = \frac{1}{\bar{\nu}_{tot}\ \sigma_{f,tot}} \sum_{x=0}^{x^{max}} \bar{E}_x\ \bar{\nu}_x\ \sigma_{f,x} \qquad (28)$$

The comparison of calculated average energies with experimental data[92-97] indicates good agreement. The dip in the $\bar{E}(E_i)$-curve above 6 MeV can be understood as an effect of second-chance fission characterized by a lower excitation energy of the fissioning nucleus (compared to first-chance fission at this incidence energy). Due to the strongly increasing probability of the second-chance contribution between 6 and 7 MeV the average post-fission neutron energy as function of E_i shows the dip, which has also been found in the experiment.

IV. CONCLUSIONS

Fission neutron spectra have been calculated within the temperature distribution model FINESSE for fissioning actinide nuclei. Due to the consideration of main fragment distributions in a rather complex form (in particular occurrence probability as function of A, Z, E^*, and TKE), prompt fission neutron emission is well described. Adjusted on the basis of ^{252}Cf(sf) data (standard spectrum as well as double-differential distribution in emission energy and angle) FINESSE in conjunction with TSM (energy partition model) is an adequate model to describe energy and angular distributions of prompt fission neutrons for any fission reaction in the actinide region. Especially the applicability to fission at any incidence energy up to about 20 MeV has to be pointed out. Experimental fission neutron spectra exists only for some actinide nuclei for few incidence energies. All calculations shown in this paper have been done in a consistent manner, i.e. on the basis of a unique parameter set as described and without any further fit. In order to avoid model uncertainties regarding optical potential, level density etc. it is proposed to apply the model with reference to the Cf standard neutron spectrum.

REFERENCES

1. B. E. Watt, Phys. Rev 87, 1037 (1952)
2. H. Märten, Proc. IAEA AGM on Nuclear Theory for Fast Neutron Nuclear Data Evaluation, Beijing, 12-16 Oct. 1987, IAEA-TECDOC-483 (1988) 1482
3. M. V. Blinov et al., Yad. Fiz. 12, 41 (1970) and Yad. Fiz. 16, 1155 (1972)
4. E. A. Seregina et al., Jad. Fiz. 43(5), 1092 (1986)
5. K. Arnold et al., Nucl. Phys. A502, 325 (1989)
6. C. Budtz-Jorgenson and H.-H. Knitter, Nucl. Phys. A490, 307 (1988)
7. H. Märten, and D. Seeliger, J. Phys. G 14, 211 (1988)
8. W. Hauser, and W. Feshbach, Phys. Rev. 87, 366 (1952)
9. J. M. Blatt, and V. F. Weisskopf, Theoretical Nuclear Physics (New York, 1952)
10. D. G. Madland, and J. R. Nix, Nucl. Sci. Eng. 81, 213 (1982)
11. H. Märten, and D. Seeliger, Nucl. Sci. Eng. 93, 370 (1986)
12. H. Märten, and D. Seeliger, J. Phys. G 10, 349 (1984)
13. W. Lang, "Nuklidausbeuten bei der Reaktion ^{235}U(n_{th},f) als Funktion der kinetischen Energie der Spaltprodukte - Ein experimenteller Zugang zur Dynamik des Spaltprozesse", Ph.D. Thesis Technische Hochschule Darmstadt, 1978
14. H. Märten, Proc. IAEA Advisory Group Meeting on Properties of Neutron Sources, Leningrad, 1986, IAEA-TECDOC-410, 144 (IAEA, Vienna, 1987)
15. R. L. Walsh, Nucl. Sci. Eng. 102, 119 (1989)
16. T. Ericson and V. Strutinski, Nucl. Phys. 8, 284 (1958), (Errata: Nucl. Phys. 9, 689 (1959))
17. H. Märten, Proc. Int. Conf. on 50th Anniversary of Nuclear Fission, Leningrad, 1989, in print
18. Y. Ando et al., Report JAERI-M83-025 (1983)
19. A. C. Wahl, Atomic Data and Nuclear Data Tables 39, 1 (1988)
20. J. Frehaut, Proc. of Cons. Meeting on Physics of Neutron Emission in Fission, Mito 1988, INDC(NDS)-220, 99 (IAEA, Vienna, 1989)
21. A. Ruben, H. Märten, and D. Seeliger, 'Energy Partition in Nuclear Fission', Present report, paper No. 2
22. S. Nair, D. B. Gayther, J. Phys. G 3 (1977) 949
23. H. Märten, A. Ruben, and D. Seeliger, Proc. Int. Conf. on 50 Years with Nuclear Fission, Gaithersburg, U.S.A., 1989, Ed. J. W. Behrens, A. D. Carlson, ANS 1989, Vol. 2, p. 274

24. B. Strohmaier and M. Uhl, Nuclear Theory for Applications, Proc. Int. Advanced Training Course on Applications of Nuclear Theory to Nuclear Data Calculations for Reactor Design, Trieste, 1980, IAEA-SMR-68/II (IAEA, Vienna, 1981) 313
25. A. V. Ignatyuk, V. M. Maslov, and A. B. Pashchenko, Sov. J. Nucl. Phys. **47** (1988) 224
26. W. Mannhart, Handbook on Nuclear Activation Data, IAEA Technical Reports Series **273** (IAEA, Vienna, 1987) 163
27. P. A. Moldauer, Nucl. Phys. **47**, 65 (1963)
28. D. Wilmore and P.E. Hodgson, Nucl. Phys. **55**, 673 (1964)
29. F. D. Becchetti and G.W. Greenlees, Phys. Rev. **182**, 1190 (1969)
30. B. Holmqvist, Arkiv Fysik **38**, 403 (1968)
31. K. Arnold, I. Düring, H. Kalka, H. Märten, A. Ruben, and D. Seeliger, Nucl. Phys. **A205**, 325c (1989).
32. H. Märten, D. Neumann, and D. Seeliger, Proc. IAEA Consultants' on on the U-235 Fast-Neutron Fission Cross-Section, and the Cf-252 Fission Neutron Spectrum, Smolenice, 1983, ed. H.D. Lemmel and D.E. Cullen, IAEA(NDS)-146/L, 199 (1983)
33. H. Märten et al., Nucl. Instr. Meth. **A264**, 375 (1988)
34. P.I. Johansson et al., Proc. Conf. on Nuclear Cross Sections and Technology, Washington, U.S.A., 1975, NBS SP **425**, 572 (1975)
35. A. Smith, P. Guenther, G. Winkler, and R. McKnight, Proc. IAEA Consultants' Meeting on Neutron Source Properties, Debrecen, 1980, INDC(NDS)-114/GT (IAEA, Vienna, 1980) 303
36. G. N. Lovtschikova et al., Proc. Int. Conf. on 50th Anniversary of Nuclear Fission, Leningrad, 1989, in print
37. H. Conde and G. Duhring, Proc. IAEA Symp. on Physics and Chemistry of Nuclear Fission, Salzburg, 1965, Vol. 2 (IAEA, Vienna, 1965) 93
38. H.-H. Knitter et al., Proc. IAEA Consultants' Meeting on Prompt Fission Neutron Spectra, Vienna, 1971 (IAEA, Vienna, 1972) 41
39. P.I. Johansson and B. Holmquist, Nucl. Sci. and Eng. **62**, 695 (1977)
40. A. B. Smith et al., Proc. IAEA Consultants' Meeting on Prompt Fission Neutron Spectra, Vienna, 1971 (IAEA, Vienna, 1972) 3
41. E.A. Alexandrova et al., At. Energ. **38**, 108 (1975)
42. S.E. Sukhikh et al., Yad. Const. **3**, 34 (1986)
43. M. Baba et al., Proc. IAEA Consultants' Meet. on the Physics of Neutron Emission in Fission, Mito (Japan), 1988, INDC(NDS)-220 (IAEA, Vienna, 1989) 149
44. R. Batchelor et al., Nucl. Phys. **65**, 236 (1965)
45. H. Märten et al.,Proc. IAEA Consultants' Meeting on Physics of Neutron Emission in Fission, Mito , 1988, INDC(NDS)-220 (IAEA, Vienna, 1989) 169
46. V. Emma et al., Nucl. Phys. **63**, 641 (1965)

Energy Partition in Nuclear Fission

A. Ruben, H.Märten, and D.Seeliger
Technische Universität Dresden, Sektion Physik
Mommsenstr.13, DDR-8027, German Democratic Republic

Abstract - *A scission point model (two spheroid model TSM) including semi-empirical temperature-dependent shell correction energies for deformed fragments at scission is presented. It has been used to describe the mass-asymmetry-dependent partition of the total energy release on both fragments from spontaneous and induced fission. Characteristic trends of experimental fragment energy and neutron multiplicity data as function of incidence energy in the Th-Cf region of fissioning nuclei are well reproduced. Based on model applications, information on the energy dissipated during the descent from second saddle of fission barrier to scission point have been deduced.*

I. INTRODUCTION

The progress achieved in nuclear fission theory have led to a qualitative understanding of most of known fission characteristics[1]. However, it fails to reproduce experimental fission data with adequate quantitative accuracy in a global manner, in particular the dependence of fission observables on excitation energy E_{cn} of the fissioning nucleus (including spontaneous fission, i.e. E_{cn}=0). One of the important questions with relevance to applications, e.g. nuclear data evaluation for actinides, is the problem of partition of total available energy (as the sum of Q-value and E_{cn}) on both complementary binary-fission fragments.

The well-known neutron multiplicity saw-tooth $\bar{\nu}(A)$ depending on fragment mass number A, which can not be understood in the framework of the liquid drop model LDM[2], has been discussed as due to shell effects by Brunner and Paul[3] and later by Vandenbosch[4].

Terrell[5] proposed a simple model to describe fission energetics as function of mass asymmetry A_1/A_2. Idealizing the scission configuration by two spheroidically shaped fragments with major semi-axis D_i, the deformation-dependent part of the potential has been minimized leading to simple expressions for describing the energy partition. The crucial parameter is the deformability α (a measure of stiffness) strongly influenced by shell effects. Based on Terrell's approach Kildir and Aras[6] studied fission energy partition for ^{252}Cf(sf). Using Myer's and Swiatecki's[7] shell correction energies δw they adjusted an empirical relation for describing α as function of δw. Corresponding α values were deduced from experimental quadrupole moments.

The static scission point model proposed by Wilkins et al.[8] is suitable to explain most of the fission characteristics. Shell and pairing effects are considered for deformed fragments (spheroids) as function of intrinsic temperature. Statistical equilibrium is separately accounted for collective degrees of freedom yielding a "collective" temperature.

The assumption of statistical equilibrium at scission was declined by Brosa[9]. His random-neck-rupture model accounts for a fissioning nucleus with a rather long neck connecting the two nascent fragment volumes. The neck cut-up is chosen randomly. This semi-stochastic approach including Raleigh's instability criterion gives a fair description of observable averages as well as width's. However, one should keep in mind that the most probable neck cut up position is determined by statics. It differs for various fission modes which are already visible in the potential energy surface.

The aim of the present work is to give a simple (and easily applicable) model for the description of average fragment energies, i.e. total kinetic energy $\overline{TKE}(A_1/A_2)$ and excitation energy $\bar{E}^*(A)$, in spontaneous as well as induced fission. Starting with a general energy balance Terrell's approach has been generalized by the incorporation of most important microscopic effects.

The model is applied to study fragment energies as function of incidence energy in comparison with experimental data. Note that $\bar{\nu}$ data are a measure of $\bar{E}^*$. Most emphasis is put to reproduce striking trends of fragment energy data in the Th - Pu region.

II. GENERAL ENERGY BALANCE IN INDUCED FISSION

Before describing the scission point model, general relations to account for the energy balance in induced fission are outlined. Fig. 1 represents a scheme of main energy values which are

important during the fission process starting at compound-nucleus excitation of energy E_{cn} and passing the double-humped fission barrier with the heights $E_{f,A}$ and $E_{f,B}$ as well as the scission point. We describe the scission point energy parts with reference to saddle B. Here, the intrinsic excitation energy is assumed to be

$$E_h = E_{cn} - E_{f,B} - \Delta_p \qquad (1)$$

with the constraint $E_h \geq 0$, i.e. E_h vanishes in the case of spontaneous and subbarrier fission. Δ_p is the pairing gap above barrier B. Its intrinsic temperature dependence is calculated according to Kristiak[10].

The potential energy release between second saddle and scission point, i.e. ΔE_{pot} is assumed to be the sum of pre-scission kinetic energy E_{pre} and dissipative energy E_{dis}. The sum $E_{dis}+E_h$ corresponds to the total intrinsic energy at scission point (E_{int}). E_{int} is distributed on the complementary fragments according to statistical assumptions (equal intrinsic temperatures, cf. paragraph 3). The basic energy balance equation

$$\bar{Q}\left(\frac{A_1}{A_2}\right) + E_{cn} = \underbrace{E_{pre} + \overbrace{E_{coul}\left(\frac{A_1}{A_2}\right)}^{F\left(\frac{A_1}{A_2}\right)} + E_{def}^{(1)} + E_{def}^{(2)}}_{\overline{TKE}\left(\frac{A_1}{A_2}\right)} + \underbrace{\overbrace{E_{dis} + E_h}^{E_{int}^{(1)}+E_{int}^{(2)}}}_{\bar{E}^*\left(\frac{A_1}{A_2}\right)} \qquad (2)$$

E_{coul} - Coulomb potential energy at scission,

$E_{def}^{(i)}$ - deformation energy of fragment i at scission,

E_{dis} - dissipative energy

$E_{int}^{(i)}$ - intrinsic excitation of fragment i at scission,

E_h - intrinsic excitation energy ("heat") at second saddle

F - potential energy at scission for given mass asymmetry

E_{pre} - pre-scission kinetic energy,

describes the partition of total available energy, i.e. sum of

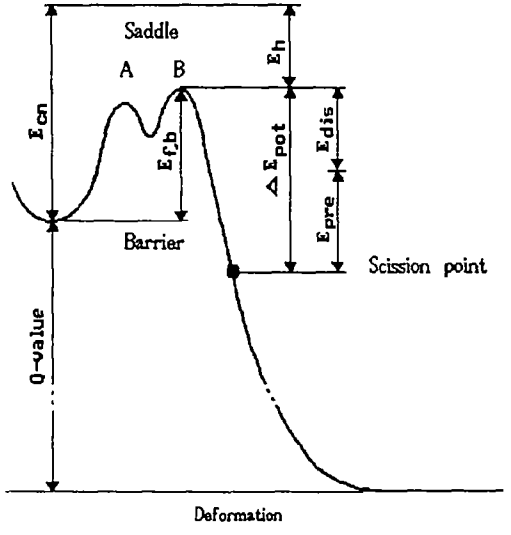

Fig.1 Potential scheme in the case of induced fission

average Q-value and fissioning nucleus excitation energy, on both fragments. E_{coul} is the coulomb potential at scission, E_{def} is the deformation energy. The "asymptotic" excitation energy of a single fragment, i.e. after dissipation of deformation energy into intrinsic energy but before de-excitation, is obtained by

$$\bar{E}^*(A_i) = E_{def}^{(i)} + E_{dis}^{(i)} \qquad (3)$$

Further, the total kinetic energy of fission fragments for given mass number ratio is given by

$$\overline{TKE}(A_1/A_2) = E_{coul}(A_1/A_2) + E_{pre} \qquad (4)$$

F denotes the deformation-dependent part of scission point potential specified in paragraph 3.

III. THE TWO-SPHEROID-MODEL

According to Terrell[5] we describe the fissioning system by two spheroidically shaped fragments nearly touching at the scission point. The nuclear forces between the fragments cause a small distance $d \approx 1.4$ fm[6]. E_{coul} is assumed to be the coulomb repulsion

energy of two charges effectively located at the centers of the fragments, i.e.

$$E_{coul} = Z^{(1)}Z^{(2)}e^2/(D^{(1)}+D^{(2)}+d) \quad . \tag{5}$$

The deformation energy is taken to be quadratic in radius change with reference to a spherical nucleus with radius $R^{(i)}$

$$E_{def}^{(i)} = \alpha^{(i)} \, (D^{(i)}-R^{(i)})^2 \tag{6}$$

($D^{(i)}$ - major semi-axis of spheroid i, $\alpha^{(i)}$ is the deformability parameter of fragment i). Minimizing the nuclear potential F in deformation space the most probable scission configuration is found. Adopting $\partial F/\partial D^{(i)}=0$ one gets a set of equations

$$E_{def}^{(i)} = \frac{E_{coul}^4}{4 \, \alpha^{(i)} \, Z^{(1)2} \, Z^{(2)2} \, e^2} \tag{7}$$

$$E_{def}^{(1)}/E_{def}^{(2)} = \alpha^{(2)}/\alpha^{(1)} \quad . \tag{8}$$

As shown by Terrell[5], the deformability parameter $\alpha^{(i)}$ is related to the stiffness parameter $C_2^{(i)}$ (quadrupole deformation) as

$$C_2^{(i)} = \frac{5}{2\pi} \, \alpha^{(i)} \, R^{(i)2} \tag{9}$$

Consequently, the deformability parameter $\alpha^{(i)}$ can be deduced in the framework of the Liquid-Drop Model[5] (LDM). However nuclear stiffness is strongly influenced by shell effects. In order to calculate effective shell correction energies $\delta w(A)$ for fragments with typical deformations at scission the following semi-empirical relation according to Kildir and Arras[6] is used,

$$\alpha(A) = \alpha_{LDM}(A) \, \frac{K-\delta W(A)}{K+\delta W(A)} \tag{10}$$

K is a constant determined by a fit of experimental stiffness data: K= (8.0 $\pm$ 0.1) MeV.

IV. PHENOMENOLOGICAL SHELL CORRECTION ENERGIES

One possible way to apply the formalism shown above is to calculate semi-empirical, i.e. effective, shell correction energies on the basis of well known fragment data. However, it should be emphasized that shell effects are washed out by intrinsic excitation. The diminution of shell correction energies due to intrinsic temperature τ at scission can roughly be described using the Bohr-Mottelson[11] relation

$$\delta w(A,\tau) = \delta w(A,\tau=0) \, \frac{t^2 \, \sinh^2 t}{\cosh t} \tag{11}$$

with

$$t = \frac{2 \, \pi^2}{\hbar \, \omega_{sh}} \, \tau \tag{12}$$

($\hbar\omega_{sh} \simeq 25 \, A^{-1/3}$ - shell energy distance[11]). According to the general energy balance (paragraph 2) the intrinsic excitation energy E_{int} includes both dissipative energy E_{dis} and heat energy above the second fission barrier E_h. The partition on the fragments is defined by the condition of equal intrinsic temperatures τ of complementary fragments at scission ($\tau^{(1)}=\tau^{(2)}$). Thus $\tau^{(i)}$ can be calculated on the basis of the Fermi-gas model approach,

$$E_{int}^{(i)}(A) = a^{(i)}(A) \, \tau^2 \tag{13}$$

The level density parameter $a^{(i)}(A)$ is described applying the Ignatyuk formalism[12] including shell effects.

Fig.2 shows the calculated phenomenological shell correction energies reduced to zero excitation at scission (τ=0) for different fission reaction. Note that these energies are very close to each other in the most probable mass region.

On the other hand, these data agree with the Strutinski-type shell energies[8] quite well. Note that the shell correction energies depicted above are only effective phenomenological quantities for fragments with averaged properties (charge, deformation, fragment energies...) without microscopic foundation.

To apply the TSM to any fission reaction a set of most reliable shell correction energies (τ=0) for $^{235}U(n_{th},f)$ and $^{252}Cf(sf)$ were determined. Interpolating these parameters and considering the

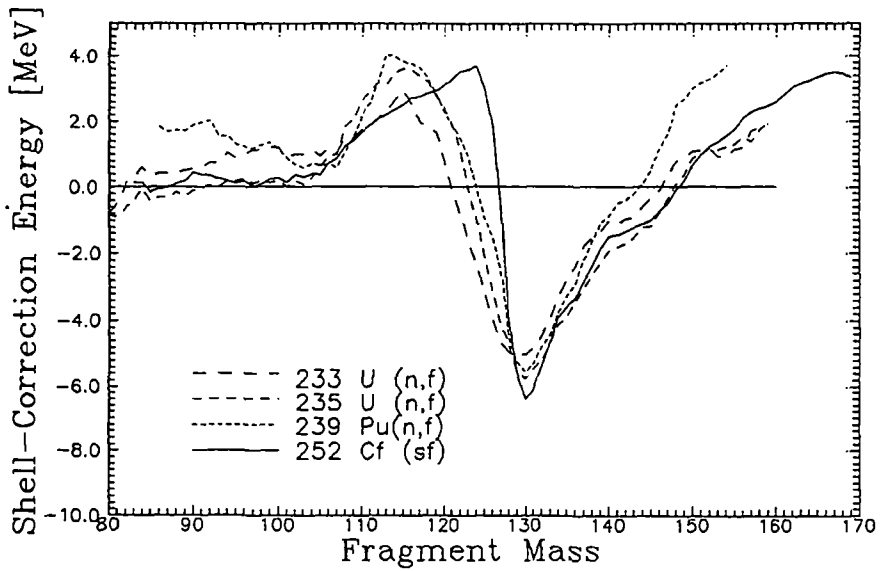

Fig.2 Calculated semi-empirical shell correction energies (τ=0) for different fission reaction ($\bar{\nu}$ data taken from ref.[24], TKE(A_1/A_2) from ref.[13,14])

intrinsic excitation, fission fragment energies and, consequently, neutron multiplicities can be obtained for any fission reaction in the actinide region.

V. DISSIPATIVE ENERGY IN SPONTANEOUS AND INDUCED FISSION

A relative vacant problem in nuclear fission is the decrease of potential energy between saddle and scission point. A wide range of possible values of the dissipative and the pre-scission kinetic energy between 0 and 50 MeV was given up to now. One method to deduce E_{dis} was presented by Gönnenwein[15]. Analyzing the proton pairing effect δ_p he has estimated dissipative energies as increasing with the fissility Z^2/A from about 3 MeV in the case of Thorium up to 11 MeV for Californium.

First applications of the TSM have shown that the calculated energy partitions are rather sensitive to the dissipated energy assumed. In deducing the phenomenological δw-parameter set this quantity is calculated according to Gönnenwein based on experimental δ_p data;

$^{235}U(n_{th},f)$: δ_p = 25 %[15] ——> E_{dis} = 6.2 MeV

$^{252}Cf(sf)$: δ_p = 12.1 %[16] ——> E_{dis} = 9.6 MeV

It has been found that an approximative parameterization of Gönnenwein's E_{dis} data for any TSM applications is not reliable. Therefore, dissipative energies have been fitted for many fissioning nuclei. These data together with the energies deduced by Gönnenwein are plotted in Fig.3 for different fission reactions.

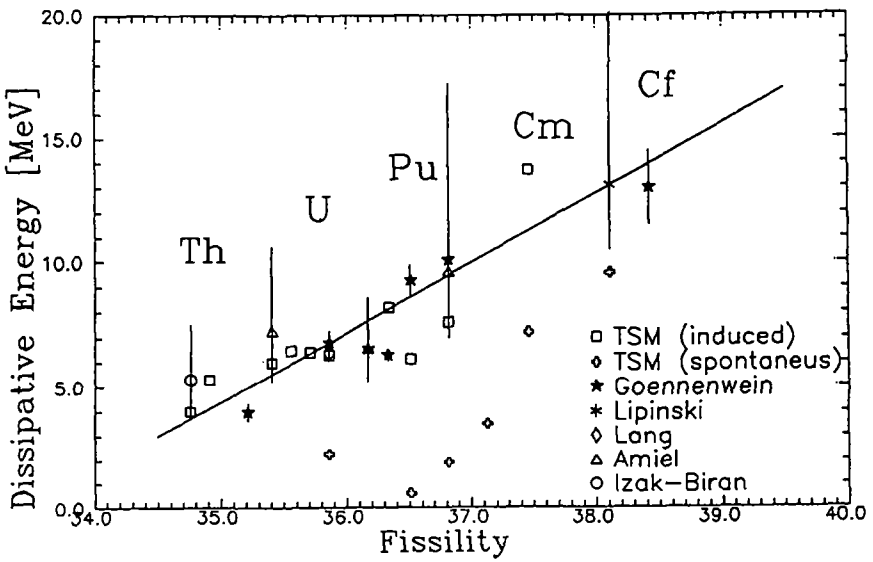

Fig.3 Fitted dissipative energies as function of fissility Z^2/A for different fission reaction in competition with the data deduced from proton odd-even effects by Gönnenwein[18] and deduced with δ_p data taken from ref.[19-22]

One might expect that ΔE_{pot} in the case of threshold fission with reference to spontaneous fission is enhanced by $E_{cn,thr}$, i.e. the compound nucleus excitation energy for threshold fission. Discussing the differences in E_{dis} and E_{pre}, we assume that the fragmentation process is separable into two phases:

1. Charge separation connected with rather strong friction: The main part of potential energy release is concentrated on E_{dis}.
2. Neck formation and rupture in conjunction with a pre-

acceleration of the nascent fragments: The potential release in this phase results E_{pre} mainly.

It is likely that differences between threshold and spontaneous (tunneling) fission concern the first phase predominantly, if ΔE_{pot} is sufficiently high. Even in this case, i.e. for $Z^2/A \geq 36$, $\overline{TKE}$ differences are very small. However for rather light fissioning nuclei ($Z^2/A \leq 36$), phase (2) is shifted close to barrier penetration in the case of spontaneous fission. E_{pre} and, consequently, $\overline{TKE}$ becomes lower compared to threshold fission.

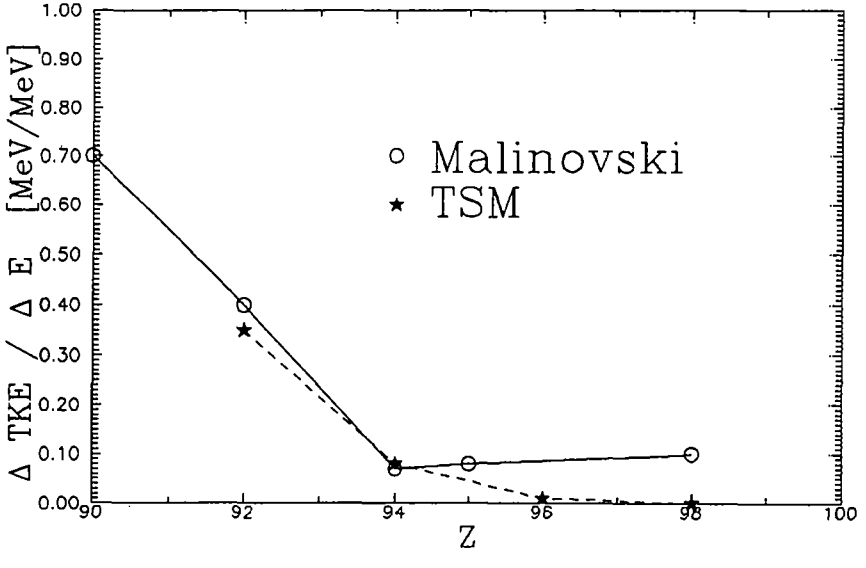

Fig.4 Change of TKE from spontaneous to threshold fission according to Malinovski[18] and fitted results obtained in the framework of TSM

Spontaneous fission compared with threshold fission exhibits a remarkable trend in changes of E_{dis} and E_{pre} (see Fig.4).
This interpretation is confirmed by the experimental-data trends. A remarkable difference in TKE between spontaneous and threshold fission, $\Delta\overline{TKE}$, exists only for nuclei lighter than Plutonium (cf. Fig.4). On the other hand, neutron multiplicity changes $\Delta\bar{\nu}$ (connected with E_{dis}) increase with the atomic mass of the fission nucleus as shown for instance by Gladkow[17].

VI RESULTS

VI.A. TOTAL KINETIC ENERGY OF FISSION FRAGMENTS

As shown in paragraph 2, the total kinetic energy as function of mass split is given by the sum of coulomb and pre-scission kinetic energy, where E_{pre} is approximated to Gönnenweins[15] values and E_{coul} is deduced from the minimization equations (equ.5,6) combined with the general energy balance (equ.1). Here, the knowledge of averaged Q-values $\bar{Q}(A_1/A_2)$ as the main part of the available energy is of special importance. These data are obtained on the basis of mass tables[23] considering an approximated charge distribution of fission fragments according to the results of Wahl[24].
The next figures show some typical examples of calculated $\overline{TKE}$ data in comparison with experimental results. Trends of changes in $\overline{TKE}$ with mass number and/or with incidence energy can be explained by the help of TSM as due to the influence of shell effects.
The total kinetic energy of two complementary fragments is essentially determined by the Coulomb repulsion. According to TSM, E_{coul} depends on the effective distance between the two fragment charges and consequently on fragment's deformation.
High negative shell correction energies (cf. Fig.2) are related to a strong stiffness. The nearly spherical shape of these fragments leads to a small distance between the charges. Thus, heavy fragments with mass number close to 132 which are characterized by extremely negative δw are connected with the maximum in $\overline{TKE}$. An increasing incidence energy diminishes this value because of decreasing stiffness due to the washing out of shell effects.
In the symmetric mass region the fragments with positive shell correction energies are quite soft concerning deformability. Since the centers of charges are far separated TKE is rather low. In this case, the diminution of shell effects is connected with smaller shell energies. Therefore, the stiffness and the kinetic energy increase with incidence energy.
The dependence of $\overline{TKE}$ on incidence energy and fragment mass is shown in Fig.5 where $\overline{TKE}$ changes $\Delta TKE(E_i,A)=TKE(E_i,A)-TKE(thermal,A)$ with reference to thermal neutron induced fission is plotted as function of fragment mass for 3 different incidence energies in the neutron induced fission of ^{235}U. The results are in good agreement with the experimental data measured by Straede[25].

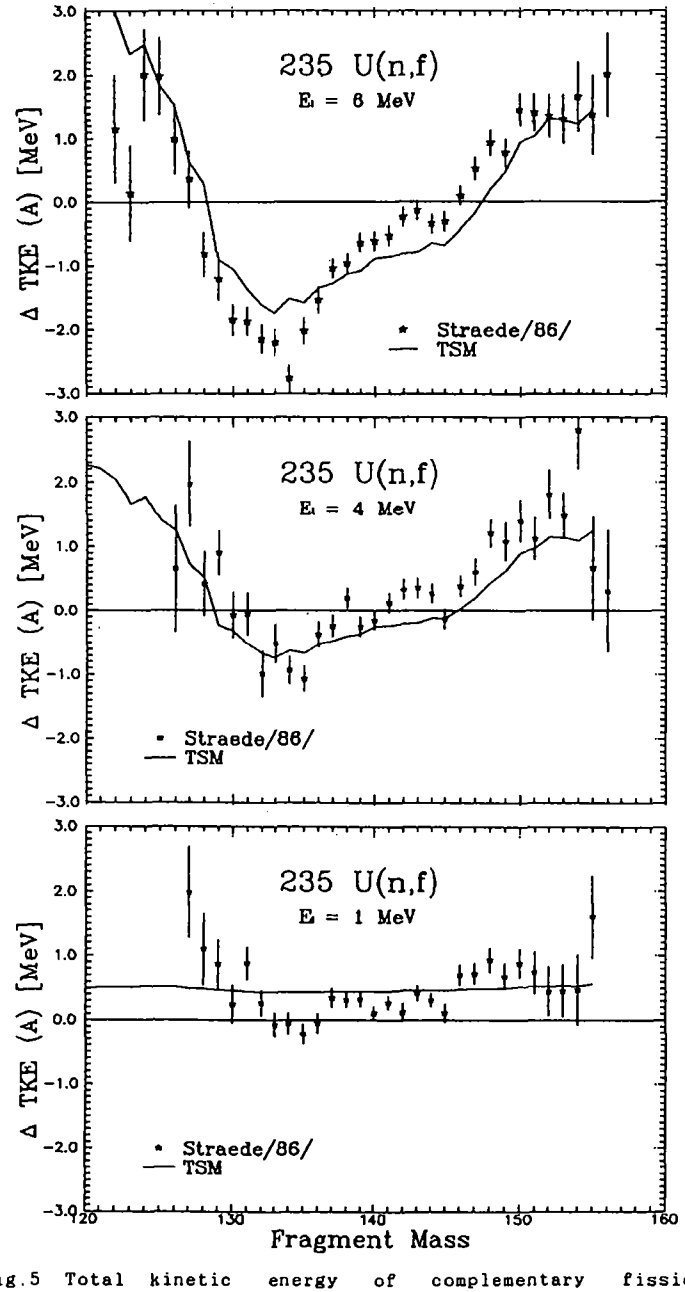

Fig.5 Total kinetic energy of complementary fission fragments of $^{235}U(n,f)$ for 3 different incidence energies plotted as difference to the value for thermal neutron induced fission (line - TSM, points - Straede[25])

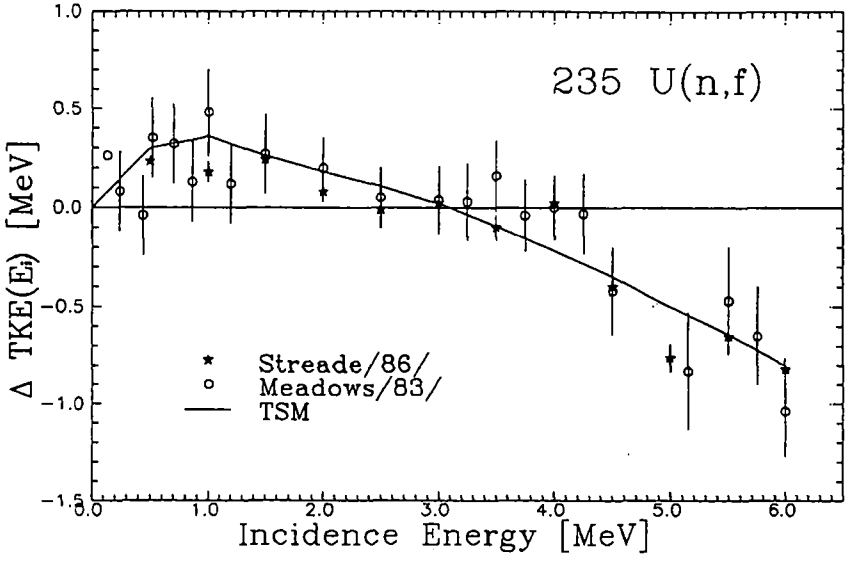

Fig.6 Averaged total kinetic energy as function of incidence energy for $^{235}U(n,f)$ plotted as difference for the value of thermal neutron induced fission. (line - TSM, points - Straede[25])

A special point to note is the general increase of TKE in the whole mass region in the case of E_i=1MeV. As shown in Fig.6 this increase is connected with a maximum of the average total kinetic energy,

$$\overline{TKE}(E_i) = \sum TKE(E_i,A_1/A_2)\ Y(E_i,A_1/A_2) \qquad (14)$$

($Y(E_i,A_1/A_2)$ - fragment mass yield) for given incidence energy. This behaviour of $\overline{TKE}$ for small incidence energy differs for various fission reactions (cf. Fig.7). In the framework of TSM, these changes in $\overline{TKE}$ are caused by alterations in the heat energy above the second fission barrier due to pair breaking. As introduced in chapter 2 (cf. Eq.2) the available intrinsic excitation energy is reduced by the pairing gap for odd-even, even-odd and especially for even-even fissioning nuclei. If the available energy above barrier, i.e. $\tilde{E}_h=E_{cn}+B_i+E_i-E_{f,b}$, is lower than the pairing gap Δ_p, the heat energy E_h is additionally reduced by Δ_p, which is a function of saddle point temperature[10]. Until the energy $\tilde{E}_h=\Delta_p$, increasing incidence energy gives rise to a higher kinetic energy of the fission fragments.

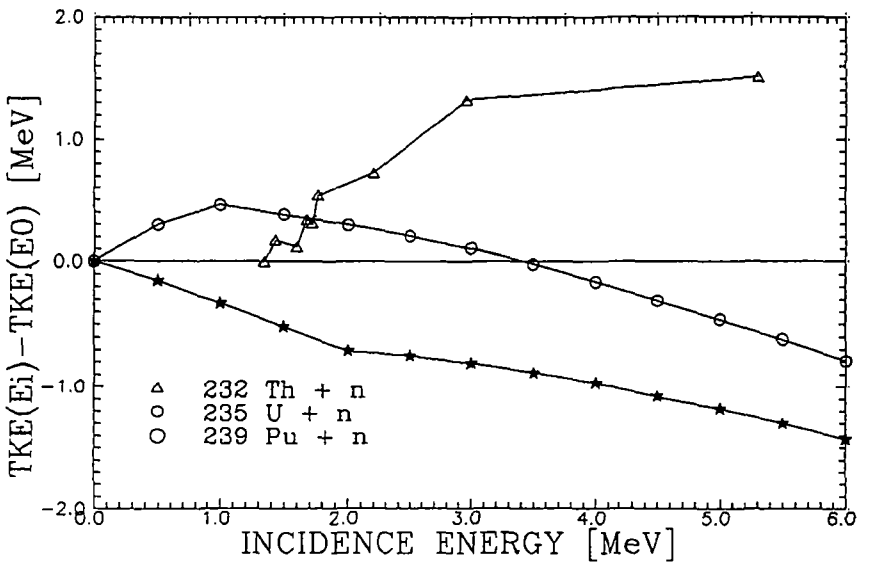

Fig.7 Calculated average total kinetic energy $\overline{TKE}(E_i)$ as difference to the value of minimum (thermal or threshold) incidence energy for different incidence energies and various fission nuclei

Above it, $\overline{TKE}(E_i)$ decrease with E_i as the result of the temperature dependence of the shell energies.

It is emphasized that the barrier structure differs for the fissioning nuclei studied in this work systematically. In particular, $E_{f,A} < E_{f,B}$ for $A \leq 235$ and $E_{f,A} > E_{f,B}$ for $A \geq 238$

The higher value determines the effective fission threshold. For the fissioning nuclei ^{233}Th, ^{236}U and ^{240}u considered in Fig. 7, the barrier values $E_{f,A}$ / $E_{f,B}$ are[26] :

6.55 / 6.65 MeV

5.63 / 5.53 MeV and

5.57 / 5.07 MeV, respectively.

Obviously, the influence of pairing on energy partition as function of incidence energy is minor or negligible, if $E_{f,A}$ is remarkably higher then $E_{f,B}$. This is the case for Pu-fission. The compound nucleus excitation energy for thermal neutron induced fission is 6.52 MeV[26] compared to the 5.07 MeV barrier B. Here, pairing at saddle doesn't play any significant role. $\overline{TKE}$ decreases as function of neutron incidence energy in the full energy range considered.

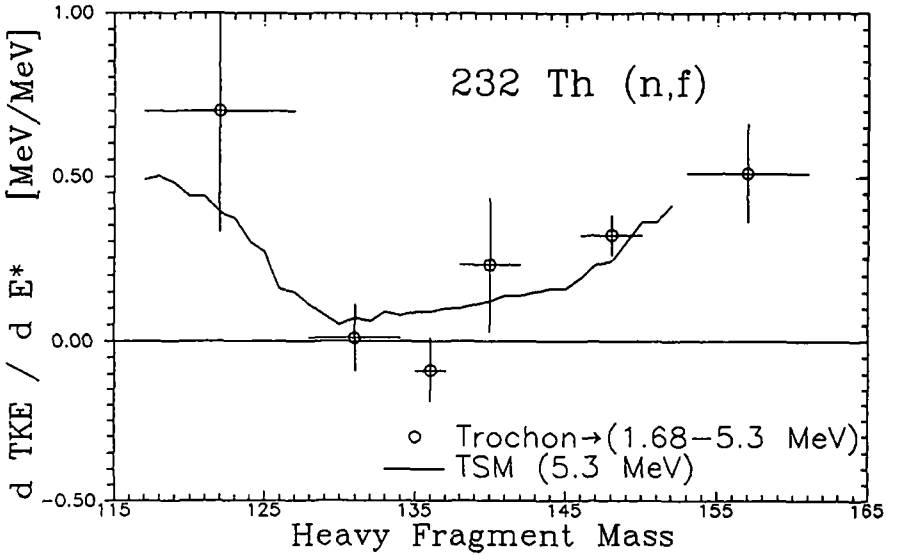

Fig.8 Total kinetic energy as difference to the value of threshold fission plotted as function of the heavy fragment mass (solid line - TSM E_i=5.8 MeV, points - averaged values for E_i= 1.72, 1.77, 2.2, 2.96 and 5.3 MeV according to Trochon[27])

The $^{232}Th(n,f)$ reaction has the opposite behaviour at low incidence energy. Further a shift of the most probable mass in the mass yield for $E_i > 3$MeV towards fragments with higher kinetic energies (cf. ref.[27]) leads to an increasing $\overline{TKE}(E_i)$ above 3 MeV incidence energy as shown in Fig.7 in the Th-case.

Fig. 8 illustrates this assumption showing the fragment mass dependence of TKE. The plotted experimental points[27] are summed values for incidence energies 1.72, 1.77, 2.2, 2.96 and 5.9 MeV.

VI.B. THE AVERAGE NEUTRON MULTIPLICITY

To deduce the neutron multiplicity of fission fragments an energy balance of fragment de-excitation is proposed including the evaporation of neutrons (multiplicity $\bar{\nu}$, average CMS energy $\bar{\varepsilon}$) and γ-ray emission (average total energy $\bar{E}_\gamma$),

$$\bar{E}^*(A_i) = \bar{\nu}(A_i)\,(\bar{B}_n(A_i) + \bar{\varepsilon}(A_i)) + \bar{E}_\gamma(A_i). \qquad (15)$$

The average neutron separation energy is calculated on the basis of mass tables[29] using an approximated charge distribution according to Wahl[24] ($\rightarrow \bar{B}_n^{z\text{-dis}}(A)$). To consider the increase of $\bar{B}_n(A)$ with $\bar{\nu}$ due to the shift of the fission fragments towards the line of β-stability these data are corrected according to,

$$\bar{B}_n(A) = \bar{B}_n^{z\text{-dis}}(A) + C\ \bar{\nu}(A) \qquad (16)$$

with the correction factor C (0.1-Uranium ...0.3-Californium).
According to the results of Frehaut[28] the average total gamma energy is assumed to be linear in the neutron multiplicity. Thus, $\bar{E}_\gamma(A_i)$ is given in the Th-Cf region by the following approximation,

$$\bar{E}_\gamma(A) = [\ G_1\ \bar{\nu}(A) + 2.2\ ]\ \text{MeV} \qquad (17)$$

The constant G_1, which depends on the mass of the fissioning nucleus as depicted in Fig. 9, is taken from Frehaut[28].
In the next figure calculated neutron multiplicities as a function of fragment mass are shown for two different incidence energies (0.8 and 5.55 MeV) for the neutron induced fission of ^{237}Np. The plotted experimental data were taken from Müller[29].
In the framework of the TSM, the saw-tooth curve of neutron multiplicity corresponds to the shell structure of the fragments. After scission the deformation energy is dissipated into excitation energy which give rise to neutron emission. Therefore, fragments with a large deformation (positive δw) cause a high number of evaporated neutrons. On the other hand the negative shell correction energies of the heavy fragments lead to a dip in the $\bar{\nu}(A)$ curve.
Both experimental and calculated data show that differences in $\bar{\nu}(A)$ with increasing incidence energy exist in the region of heavy fragments (125<A<145) mainly. As shown in Fig.2 these fragments are characterized by extremely (negative) shell correction energies which are especially changed due to intrinsic excitation.
A last remarkable test of the accuracy of description of energy partition and neutron emission with the TSM is the dependence of neutron multiplicity averaged over all fragments on incidence energy. The last three figures show this behaviour for three different fission reactions. In the case of Thorium (Fig.11) this investigation includes both (n,f) and (n,n'f) reactions. To account for multiple chance fission, in general (n,jnf), the

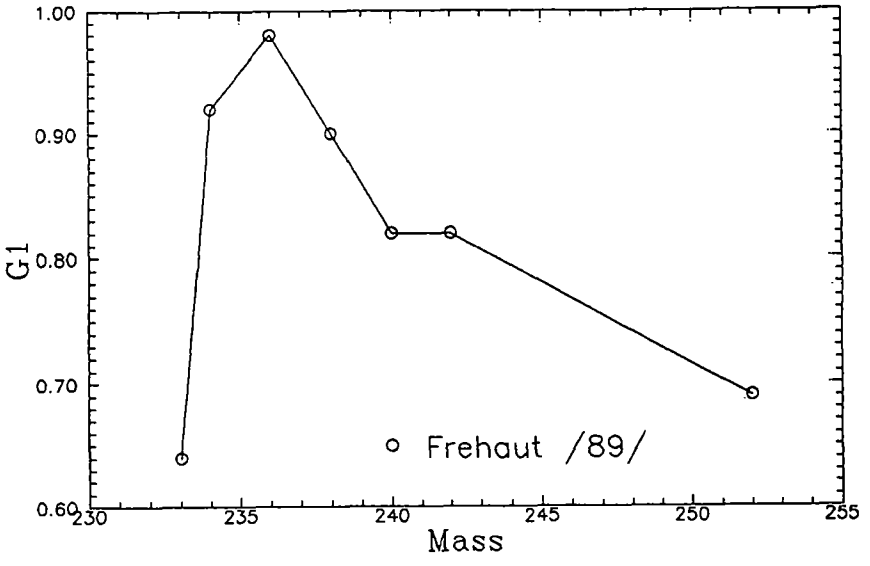

Fig.9 Constant G_1 for relation between average total γ-energy and average neutron multiplicity as function of mass of fissioning nucleus according to Frehaut[29]

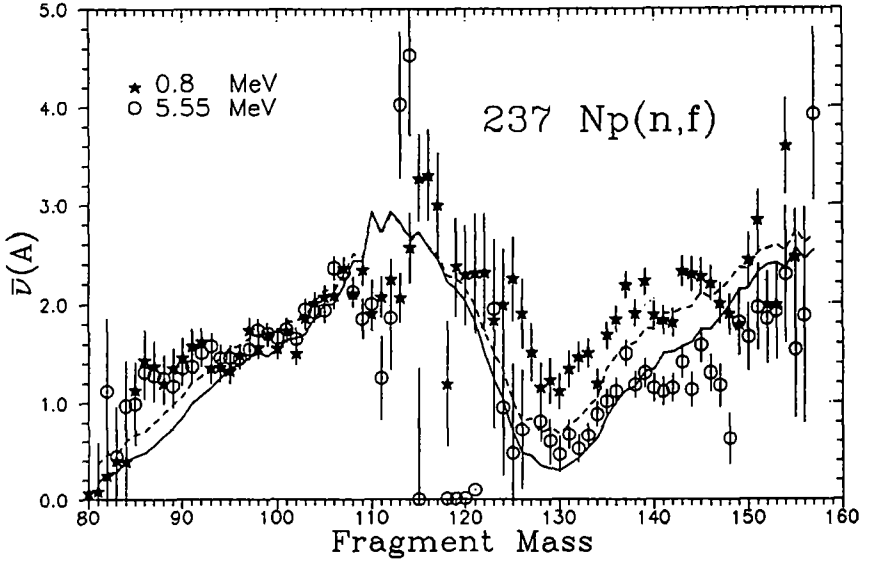

Fig.10 Calculated neutron multiplicity as function of fragment mass in comparision with experimental data[29] for the ^{237}Np(n,f) reaction

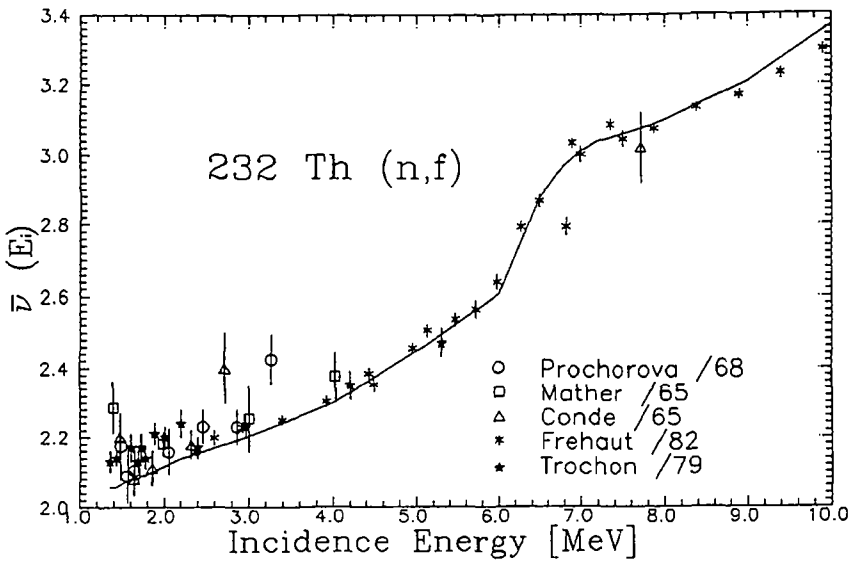

Fig.11 Average neutron multiplicity as function of incidence energy for the neutron induced fission of ^{232}Th (experimental data were taken from ref.:[27,90-96])

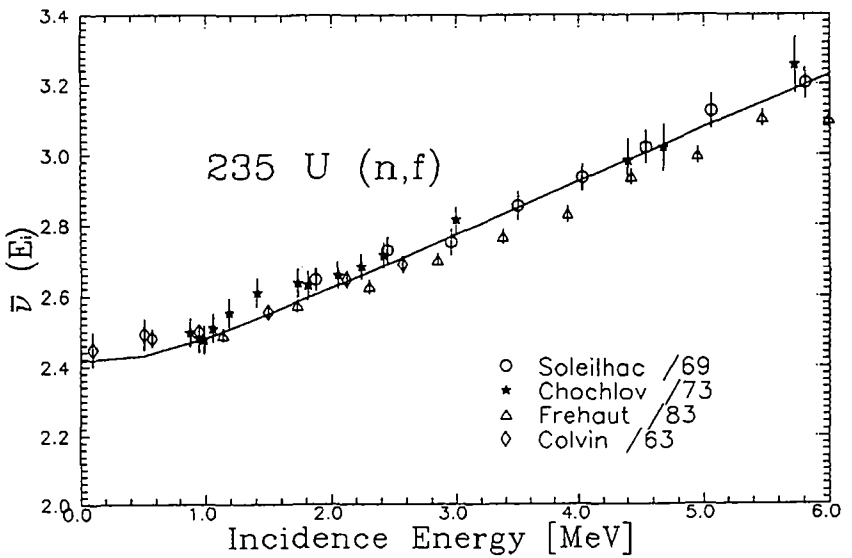

Fig.12 Average neutron multiplicity as function of incidence energy for ^{235}U(n,f) (experimental data were taken from ref.[89-96])

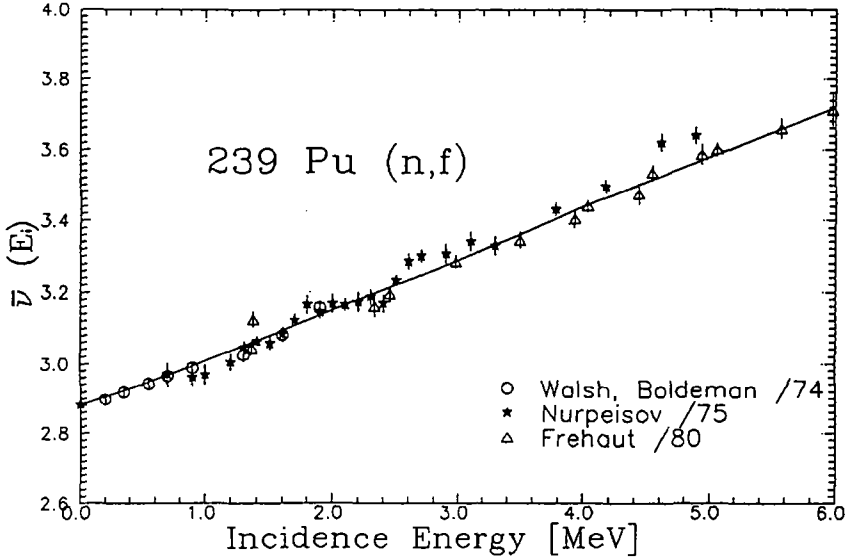

Fig.13 Average neutron multiplicity as function of incidence energy for ^{239}Pu(n,f) (experimental data were taken from ref.[87-89])

neutron multiplicities $\bar{\nu}_j(E_i)$ for both reactions have been calculated and added considering the partial fission cross sections $\sigma_{f,j}(E_i)$ of chance j,

$$\bar{\nu}_{tot}(E_i) = \frac{\sum_{j=0}^{j_{max}} \bar{\nu}_j(E_i)\ \sigma_{f,j}(E_i)}{\sigma_{f,tot}} \qquad (17)$$

The bend in the $\bar{\nu}(E_i)$ curve above 6 MeV incidence energy is a consequence of second chance fission characterized by lower $\overline{TKE}$ as in the first chance case and consequently, higher $\bar{\nu}$ values. The TSM calculation reproduces the experimental data.

Fig. 12 and 13 show a similar investigation as discussed above for neutron induced fission of ^{235}U and ^{239}Pu for the first chance emission (n,f). Even these figures show a good agreement between measured and calculated data.

VII. SUMMARY AND CONCLUSIONS

The TSM as a scission point model with semi-empirical, temperature-dependent shell correction energies for deformed fragments at scission is successful in describing the main features of energy partition in fission as function of mass asymmetry. The diminution of shell effects due to scission point temperature, which depends on the dissipated energy as well as incidence energy (influenced by pairing effects), cause considerable changes of fragment energies as function of incidence energy.

Remarkable changes in the fragment energies between spontaneous and threshold fission are explained by the TSM as an effect of systematic alterations in the dissipated and pre-scission kinetic energy. Fitting the calculated fragment data dissipative energies for both types of fission reaction have been obtained.

The average fragment excitation energy has been used used to obtain neutron multiplicity by the help of an energy balance of fragment de-excitation, which includes neutron evaporation and γ-ray emission. The typical saw-tooth in the $\bar{\nu}(A)$ curve as well as the dependence of $\bar{\nu}$ on incidence energy is reproduced by the TSM with good accuracy.

The TSM provides the basis for several applications as the calculation of fragment data as well as neutron emission probabilities. This model will be used for corresponding data systematics in next future.

REFERENCES

1. J. Moreau and K. Heyde, manuscript "Theoretical models of mass distributions", to be published in "Nuclear Fission Review", ed. by C. Waagemans
2. N.Bohr and J.Wheeler, Phys. Rev 56, 426 (1939)
3. W.Brunner and H.Paul, Ann.d.Phys.7, 326 (1961)
4. R.Vandenbosch, Nucl.Phys.46, 129 (1963)
5. J. Terrell, Proc. IAEA Symp. on Phys. and Chem. of Fission, Salzburg, 1965 (Vienna, 1965) Vol. II, p. 3
6. M. Kildir and N.K. Aras, Phys. Rev. C25, 365 (1982)
7. W.D.Myers and W.J.Swiatecki, Nucl.Phys.81, 1 (1966)
8. B.D. Wilkins et al., Phys. Rev. C14, 1832 (1976)
9. U.Brosa et al., Proc. XVIth Int. Symp. on Nucl. Phys., Gaussig (GDR), 1986, ZfK-610, 162 (1986)
10. J. Kristiak, Proc. 5th Int. Symp. on Neutron Induced Reactions, Smolenice, 1988, in print
11. A. Bohr and B.R. Mottelson, "Nuclear Structure" (Benjamin, New York, 1975), vol. II
12. A. V. Ignatjuk et al., Yad. Fiz. 42 /, 569 (1985)
13. W. F. Apalin et al., Nucl. Phys. 71, 553 (1965)
14. R. Schmidt-Fabian, PhD Thesis,"Messung der spontanen Spaltung von ^{252}Cf am Darmstadt - Heidelberger - Kristallkugel - Spektrometer", (1988) Ruprecht-Karls-Universität Heidelberg
15. F. Gönnenwein et al., Proc. XVIIth Int. Symp. on Nucl. Phys., Gaussig (GDR), 1987, ZfK-646, 129 (1988)
16. T. Datta et al., Proc. XVIIIth Int. Symp. on Nucl. Phys., Gaussig (GDR), 1988, in print
17. W. W. Gladkov et al., Yad. Const. 1(40), 48 (1981),
18. W. W. Malinovski, Jad. Konst. 2, 25 (1987),
19. R. J. Lipinsk and B. W. Wehring, Phys.Lett. 66B, 326 (1977)
20. W. Lang, PhD Thesis, "Nuklidausbeuten bei der Reaktion ^{235}U(n_{th},f) als Funktion der kinetischen Energie der Spaltprodukte - Ein experimenteller Zugang zur Dynamik des Spaltprozesses", TH Darmstadt (1979)
21. S. Amiel et al., Phys. Rev. C15, 2119 (1977)
22. T. Izak-Biran and S. Amiel, Phys. Rev. 96, 1059 (1954)
23. Y. Ando et al., JAERI-M83-025
24. A. C. Wahl, Atomic Data and Nuclear Data Tables 39, 1 (1988)
25. C. A. Straede et al., Nucl. Phys. A462, 85 (1987)
26. S. Bjornholm and J. E. Lynn, Rev. Mod. Phys. 52, No.4, 725 (1980)
27. J. Trochon et al., Nucl. Phys. A318, 63 (1979)
28. J. Frehaut, Proc. of Cons. Meeting on Physics of Neutron Emission in Fission, Mito 19888, IAEA Wien, 1989, INDC(NDS)-220, 99
29. K. Müller et al., "Numerical results of a (2E,2v) - measurement for fast neutron induced fission of ^{235}U and ^{237}Np", KFK - Berichte 3220 (1981)
30. L. I. Prochorova et al., Sov. J. Nucl. Energy 7, 579 (1968)
31. D. S. Mather et al., Nucl. Phys. 66, 149 (1965)
32. H. Conde et al., Arkiv Phys. 29, 33 (1965)
33. J. Frehaut et al., Proc. of Intern. Conf. on Nucl. Data for Science and Technology, 6-10 Sept. 1982, Antwerpen D. Reidel Publishing Company, 78 (1983)

34. M. Soleilhac et al., Nucl. Energy 23, 257 (1969)
35. J. A. Chochlov et al., Proc. IIIth Conf. on Neutron Phys., Kiev, 9-13 June, ZNII Atominform, V, 186 (1976)
36. D. W. Colvin and M. G. Sowerby, in R. J. Howerton, Nucl. Sci and Eng., 62, 438 (1977)
37. B. L. Walsh and J. W. Boldeman, Ann. Nucl. Sci. Engng. 1, 353 (1974)
38. B. Nurpeisov et al., At. Energy 39 /3, 199 (1975)
39 J. Frehaut et al., "Recent results on ν-prompt measurements between 1.5 and 15 MeV", Paris 1980

Prompt Fission Neutron Spectra and Fragment Characteristics for Spontaneous Fission of even Pu - Isotopes

H. Märten, A. Ruben, D. Seeliger
Technische Universität Dresden
Mommsenstr.13, DDR-8027, German Democratic Republic

Abstract: *A phenomenological scission point model including temperature-dependent shell effects has been used to solve the energy partition problem as function of mass asymmetry for Pu-fission. Relevant fragment data were used as the basis for applying a temperature-distribution model, which yields neutron multiplicity, energy and angular distribution of prompt fission neutrons. Calculated data for ^{238}Pu, ^{240}Pu, and ^{242}Pu are presented and discussed in comparison with experimental data.*

1. Introduction

As emphasized in refs.[1,2], fission neutron data for spontaneously fissioning Pu-isotopes are relevant to nuclear safeguards, e.g. for neutron coincidence counting techniques applied to Pu-assay systems. However, experimental data on energy spectra are scarce. They exhibit remarkable uncertainties.
In this work , we consider the calculation of fission neutron data for even Pu-isotopes as a typical example of applying a theoretical model to describe nuclear data without a sufficient experimental data base for model parameter variation.
Recently Walsh et al.[3] have analyzed the Pu fission neutron spectra on the basis of the Madland-Nix model (MNM) including emission anisotropy in the center-of-mass system (the so called "spin-dependence"). Since this model relies on a reduction of the fragment parameter space in fact , an intricate distribution in mass and charge number A, Z, total kinetic energy TKE, excitation energy E^*, angular momentum I, etc. to a representative fragment pair, it is easily applicable to any fission reaction.
As discussed in refs.[3-6], the physical consistency of a fission neutron model can be understood as "internal" (concerns the emission model applied to a fragment diversity described by a given fragment distribution) as well as "external" (concerns the description of the fragment distribution for any fission reaction) consistency.
Based on studies within a complex cascade-evaporation model[7,8] and a Hauser-Feshbach-calculation[2] with explicit consideration of fragment spin[8] the complex temperature-distribution model FINESSE[9] has been developed. It relies on basic ideas of the MNM as well as its generalized version[10]. FINESSE involves a realistic temperature distribution of the fragments as function of mass number. The description of the fragment parameter sets necessary within FINESSE, i.e. $\overline{E^*}(A)$, $\overline{TKE}$ (A_1/A_2), mass yield Y(A), etc., is done on the basis of a phenomenological fission theory (e.g. the two- spheroid model TSM[11]).
Pu fission data, as $\overline{TKE}$ (A_1/A_2)[12-15], Y(A)[12-14], Y(A,TKE)[13] and $\bar{\nu}_{tot}$[2,16] have been measured in the last years by several groups. These results are considered as basis for the comparison with calculated fragment data. It should be emphasized that even for the Pu-isotopes studied in this work Wagemans et al.[13] found a remarkable influence of neutron number of the fissioning nucleus on the yield of fission modes (cf. refs.[17,18]).
One of the open questions is the dependence of neutron multiplicity on mass number $\bar{\nu}(A)$, which hasn't yet been measured. This quantity as a measure of $\overline{E^*}(A)$ is strongly correlated to the shape of the fission neutron spectrum. $\bar{\nu}(A)$ should show a saw-tooth behaviour as typical in the Th-Cf region of fissioning nuclei. However, the quantitative characteristic of the dependence is strongly influenced by shell effects and, consequently, correlated to fission mode yields. Thus, it is obvious that the applied purpose of the present work is strongly connected with some fundamental questions of fission physics at low (or even zero) excitation energy of the fissioning nucleus.

2. The Model Complex TSM - FINESSE

2.1. Phenomenological fission model (TSM)

As described in ref.[11] in more detail, the TSM is a scission point model including temperature-dependent, semi-empirical shell correction energies δw of deformed fragments at scission.
Applying the TSM including potential energy minimization at scission (in regard to variation of fragment deformation), shell energy data have been deduced from fragment data for well-investigated fission reactions as ^{252}Cf(sf) and ^{235}U(n_{th},f).
It has been found that the dependence δw (A) is quite similar for fissioning systems in the Th-Cf region. Thus it has been concluded that the use of these shell energy data sets (reduced to zero

temperature) to determine the $\delta w(A)$ function for the actual fission reaction by interpolation is justified.

The TSM energy balance includes dissipative energy as well as pre-scission kinetic energy. The first one has been adjusted for many fissioning systems in the Th-Cf region. Systematic differences between spontaneous fission and threshold fission have been found. The empirical dissipative energies (3.5 MeV, 1.9 MeV, and 0.6 MeV for ^{238}Pu, ^{240}Pu, and ^{242}Pu, respectively) have been used in this work. Within TSM, $\overline{TKE}$ (A_1/A_2) is considered as the sum of Coulomb potential at scission and pre-scission kinetic energy. The average excitation energy of an individual fragment is given by its deformation energy at scission point (which dissipates into internal excitation within about 10^{-20}s) as well as by a certain part of intrinsic excitation energy at scission (i.e. the sum of dissipative energy and the excitation energy of the fissioning system at the second saddle of the double-humped fission barrier). The latter one is estimated by statistical assumptions. Assuming unique temperature of the scissioning system, the ratio of excitation energy of both complementary fragments at scission is given by the inverse ratio of level density parameters (also influenced by shell energy).

Based on the $\bar{E}^*(A)$ data, $\bar{\nu}(A)$ can easily be estimated by a further energy balance concerning fragment de-excitation as due to neutron and γ-ray emission mainly. Here, the correlation between $\bar{\nu}$ and the average total γ-ray energy and the increase of neutron separation energy during a neutron emission cascade are taken into account, see ref. [11],

$$\bar{E}^*(A_i) = \bar{\nu}(A_i)\,(\bar{B}_n(A_i) + \bar{\varepsilon}(A_i)) + \bar{E}_\gamma(A_i). \qquad (1)$$

$$\bar{B}_n(A) = \bar{B}_{n,o}(A) + C\,\bar{\nu}(A) \qquad (2)$$

$$\bar{E}_\gamma(A) = [\,G_1\,\bar{\nu}(A) + 2.2\,]\ \text{MeV}\ . \qquad (3)$$

2.2. Statistical-model approach to prompt neutron emission (FINESSE)

Neutron evaporation from fully accelerated fragments is considered as the predominant mechanism of fragment de-excitation. This assumption has been verified in several recent studies (cf. ref. [8]).

In order to derive a tractable fission neutron model, which can be applied to any fission reaction in connection with TSM, the full-scale distribution $P(A,Z,TKE,E^*,I)$ of fission fragments is reduced to:

(i) a distribution $P(E^*,A)$, which is transformed into a distribution in rest-nucleus temperature T resulting in P(T:A) (considering cascade emission),

(ii) an A-dependent charge distribution P(Z:A) to derive averaged structure data as neutron binding energy,

(iii) averages $\overline{TKE}$ (A_1/A_2) as basis for the transformation of center- of-mass system (CMS) spectra into laboratory system (LS) distributions,

(iv) total average $\bar{I}$ giving rise to a CMS anisotropy, which is considered in dependence on CMS energy as in [10].

An extended Weisskopf ansatz is applied to calculate the CMS spectrum for given T, i.e.

$$\varphi(\varepsilon:T) \sim \varepsilon\,\sigma_{inv}(\varepsilon)\,\exp\left\{-\frac{\varepsilon}{T} - \frac{\varepsilon^2}{4aT^3}\right\} \qquad (4)$$

This equation accounts for the second-order term of the entropy expansion in powers of energy.

Assuming a Gaussian distribution in initial excitation energy the total distribution in U (rest-nucleus excitation energy) is very well approximated by

$$P(U:A) = \frac{1}{1 + \exp\left[\dfrac{U - \hat{U}(A)}{d(A)}\right]} \qquad (5)$$

(d - "diffuseness" parameter, $\hat{U}$ - "edge" parameter).. P(U:A) yields the temperature distribution P(T:A) directly via transformation on the basis of Fermi-gas model relation $U=a(A)T^2$. In contrast to MNM, where an idealized P(T) shape is assumed, this procedure results in a more realistic distribution in T. Further, effective a(A) values for fission fragments are used [9].

Finally, we obtain the CMS spectrum of fission neutrons by

$$\varphi(\varepsilon:A) = \int_{T_o}^{*} K(T:A)\,P(T:A)\,\varphi(\varepsilon:T,A)\,dT \qquad (6)$$

K(T) normalizes eq.(6) to 1. The value T_o, the lower limit for integration over T, has been introduced to account for competition between neutron and γ-ray emission approximately.

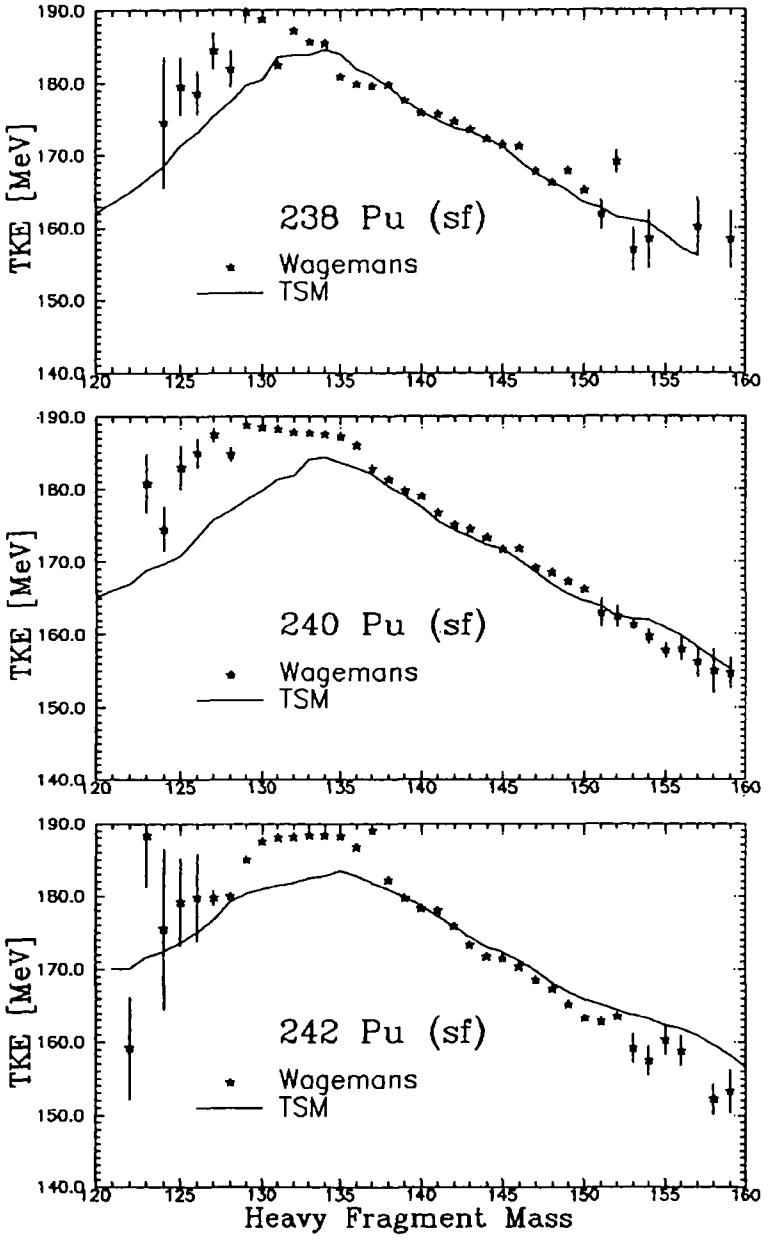

Fig. 1 Calculated total kinetic energy (lines) as function of heavy fragment mass number for spontaneous fission of Pu-isotopes in comparison with experimental data of Wagemans et al[14]

After transformation of double-differential CMS distribution in emission energy and angle into LS yielding $N(E,\Theta:A)$ (E - LS emission energy, Θ - LS angle of neutron emission with reference to light fragment direction), we obtain the total distribution by

$$N(E,\Theta) = \sum_A P(A)\, N(E,\Theta:A)\cdot\bar{\nu}(A) \qquad (7)$$

The mass yield curves P(A) for Pu-isotopes have been taken from ref.[14].

3. Results

3.1 Fission Fragment Characteristics

Fig.1 represents the calculated total kinetic energy as function of mass asymmetry. Compared with the measured data of Wagemans[13] there is a rather good agreement for heavy-fragment mass-number $\gtrsim$ 135. In the case of more symmetric fission there are remarkable deviations, which should be interpreted as due to the influence of the high-yield fission mode with $\bar{A}_H \approx 130$. Since the mass yield curves have their maxima at A_H close to 140, $\overline{TKE}$ values (averaged over A) calculated within TSM agree with measured data (table 1).

Tab.1 Fissility parameter, total neutron multiplicity, and total kinetic energy for even Pu-isotopes

Reaction	$\frac{Z^2}{A}$	$\bar{\nu}_{tot}$		TKE	
		measured	TSM	measured	TSM
^{238}Pu(sf)	37.13	2.21[16]	2.205	176.5[13]	177.2
^{240}Pu(sf)	36.82	2.156[2]	2.167	179.1[13]	177.9
^{242}Pu(sf)	36.51	2.145[2]	2.160	180.4[13]	178.5

In Fig.2 the fragment mass dependence of the average neutron multiplicity is shown for the Pu fission reactions studied in this work. The small differences between the curves are caused by the general increase of $\bar{\nu}$ with fissility (Z^2/A). Total neutron multiplicities exhibit the same trend (table 1).

The good agreement of measured and calculated $\bar{\nu}_{tot}$ is of special importance for the calculation of the prompt fission neutron

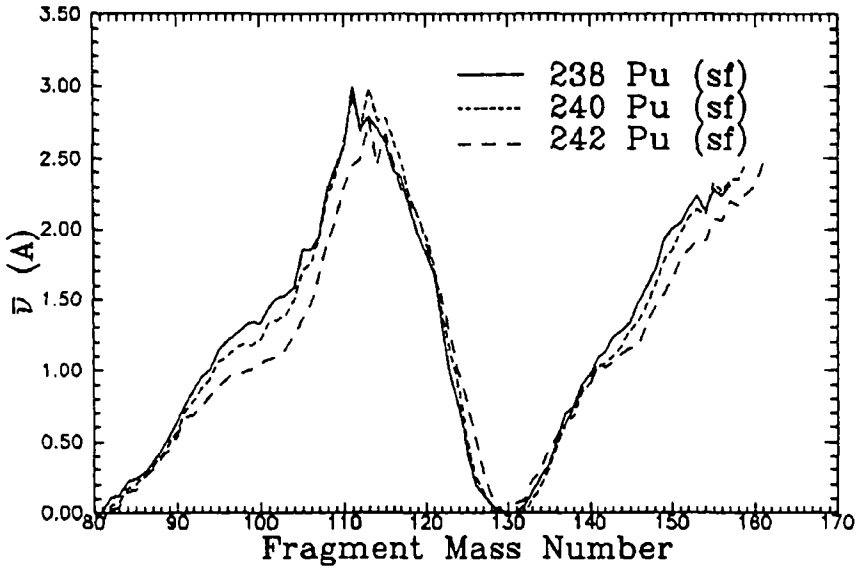

Fig. 2 Average neutron multiplicity calculated within TSM as function of fragment mass for the spontaneous fission of the Pu-isotopes

spectra because of the strong influence of the fragment excitation energy (correlated with $\bar{\nu}$) on the temperature distribution P(T).

3.2. Prompt fission neutron spectra

Based on the fragment data ($\bar{E}^{*}(A)$, $\overline{TKE}$ (A_1/A_2), P(A)) discussed in paragraph 2., the prompt fission neutron distribution spectra $N(E,\Theta)$ have been calculated within FINESSE. The integral spectra N(E) are represented Figures 3-5 as deviation from a Maxwellian.

$$D(E) = \left(\frac{N(E)}{M(E)} - 1 \right) 100\ \% \qquad (8)$$

The temperatures T_M of these Maxwellian distributions M(E) have been deduced from the average neutron energies ($T_M = 2/3\ \bar{E}$).
Note, that the calculated Maxwellian temperatures, which are representative for the spectrum in the whole energy region, may differ from those found in experiment. Experimental data (as for ^{240}Pu(sf)) are available for a limited energy range (about 2-12 MeV). Due to the spectral shape of fission neutron spectra (see Fig.3), Maxwellian temperatures deduced from experimental data are

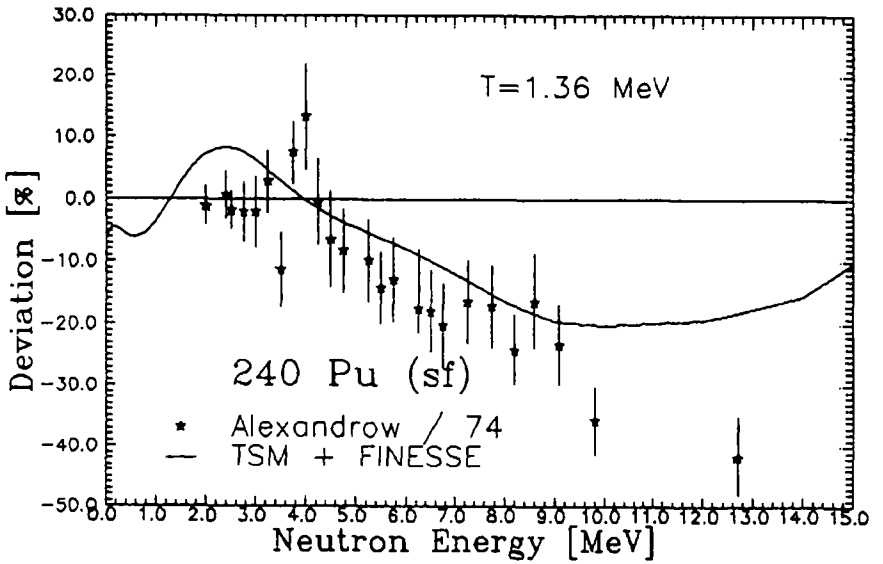

Fig. 3 Calculated fission neutron spectrum of ^{240}Pu(sf) shown as percentage deviation from a Maxwellian with T_M=1.36 in comparison with experimental data taken from ref.[19] renormalized to the FINESSE T_M

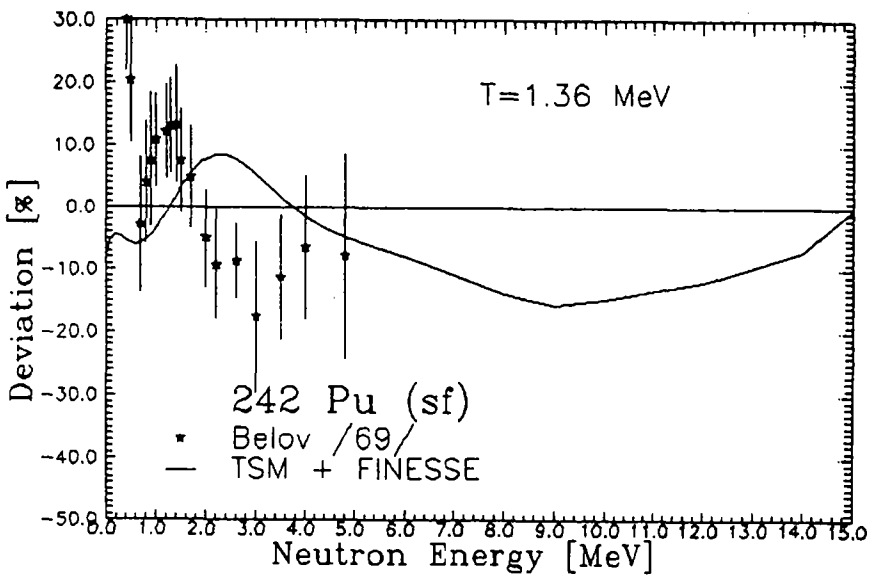

Fig. 4 Calculated fission neutron spectrum for ^{242}Pu(sf) shown as deviation from a Maxwellian with T_M=1.36 in comparison with experimental data taken from Belov[22]

systematically lower than value representing the whole spectrum. Further, the uncertainty of experimental data and, consequently, of the Maxwellian temperatures are rather high.As shown in Fig.3 there is a good agreement between the calculated and measured spectra (Alexandrova[19]) up to 10 MeV emission energy for ^{240}Pu(sf).The shape of the ^{242}Pu(sf) spectrum measured by Belov et al.[22] doesn't correspond to systematics in the Th-Cf region. As shown in Fig.4 the agreement between experimental data and the TSM-FINESSE calculation is moderate.In Fig. 5, the calculated spectrum for ^{238}Pu(sf) is represented. For this reaction, experimental data does not exist. An important question for many applications is the ratio of the emission spectra of the Pu-isotopes studied in this work. As depicted in Fig. 6 both the ^{238}Pu(sf) and the ^{242}Pu(sf) spectra are enhanced with reference to the ^{240}Pu(sf) spectrum in the high energy range. For the ^{238}Pu-isotope, this is caused by the higher fragment excitation energies which correspond to the relative high neutron multiplicity (cf. Tab.1).For ^{240}Pu(sf) and ^{242}Pu(sf) the fragment excitation energies are quite similar.

However, a shift in the fragment mass yield towards symmetric fission in the case of ^{242}Pu(sf) favors higher excited light

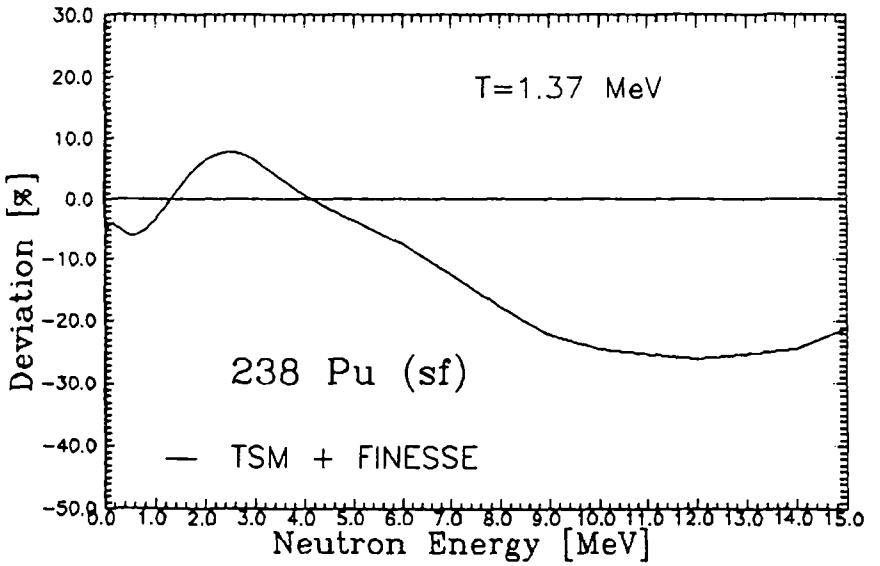

Fig. 5 Calculated fission neutron spectrum of ^{238}Pu(sf) shown as deviation from a Maxwellian with T_M=1.37

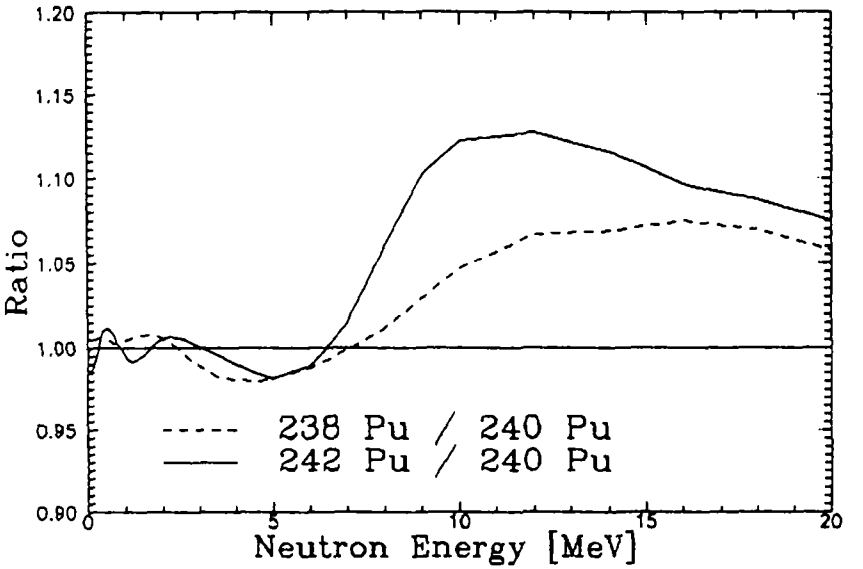

Fig. 6 Ratio of the calculated spectra of ^{242}Pu(sf) and ^{238}Pu(sf) to ^{240}Pu(sf)

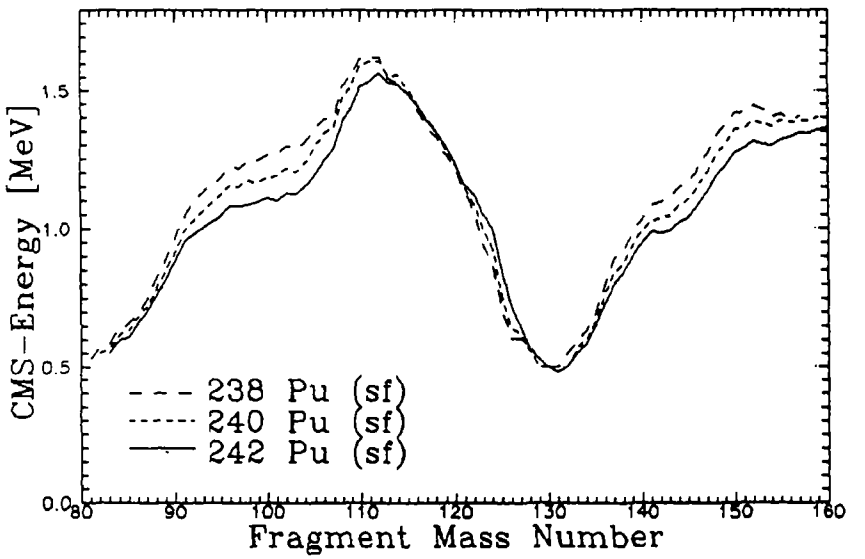

Fig. 7 Average CMS-neutron energy as function of fragment mass for the spontaneous fission of Pu-isotopes

fragments (around A=108). These remarks are supported by Fig. 7, where average neutron energies of CMS emission spectra are plotted versus fragment mass. The spectrum ratios calculated in this work do not correspond to the results of Walsh et al.[3]

3.3 Angular distribution of the neutron emission spectra

In the framework of FINESSE, both energy and angular distributions of neutron emission in nuclear fission are calculated. Angular anisotropy in the laboratory system (with reference to the direction of the fission axis) is described by

$$R(E) = \frac{N(E,\Theta = 0^\circ) + N(E,\Theta = 180^\circ)}{2\, N(E,\Theta = 90^\circ)}$$

as function of neutron energy. As shown in Fig. 8 all fission reactions are characterized by a similar strong increase of anisotropy with neutron emission energy. The small differences of R(E) curves of Pu-isotopes at high energy are a consequence of different average CMS energies (cf. Fig.8).
This should be interpreted in connection with calculated total neutron multiplicity $\bar{\nu}_{tot}$. Whereas our calculations are in good

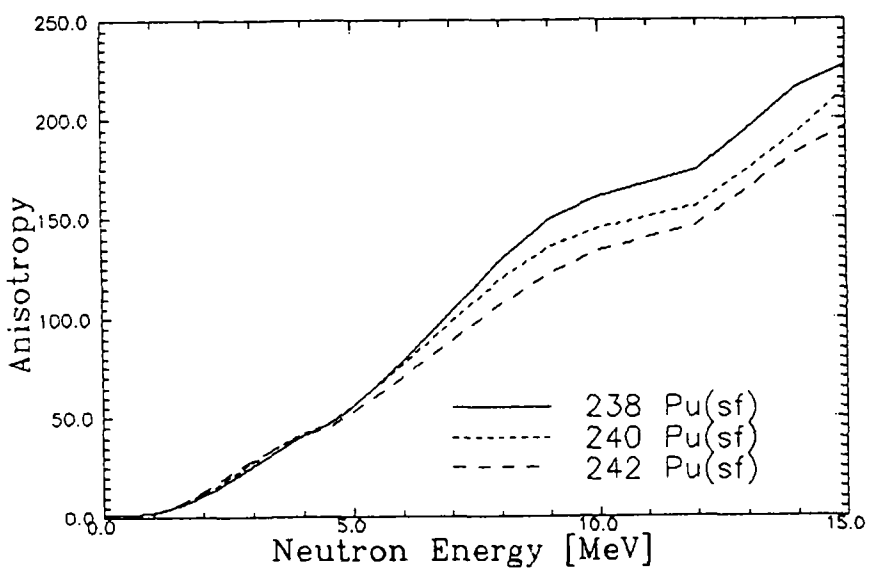

Fig. 8 Calculated anisotropy of the emission spectra as function of neutron energy in the laboratory system for spontaneous fission of even Pu-isotopes

agreement with experiment (within $\lesssim$ 0.7%), the calculations by Walsh differ from experiment by $\lesssim$ 10%

4. Summary

In the framework of the model-complex TSM/FINESSE, fission fragment characteristics and neutron emission spectra for spontaneous fission of even Pu-isotopes have been predicted. The total kinetic energies and the average neutron multiplicities are in good agreement with measured data. The calculated prompt fission neutron spectra as representative for the whole energy range point at a higher average neutron energy than deduced from experiment for a limited energy range. Remarkable deviations of our calculations from the theoretical results by Walsh et al.[3] have been found. It has been shown that the fragment data calculated within TSM are in good agreement with experiment even in most probable mass number range. These data are assumed as a reliable basis for the FINESSE calculation. In contrast to Walsh et al.[3] $\bar{\nu}_{tot}$ values are very well reproduced. Since $\bar{\nu}_{tot}$ is a measure for the total average excitation energy (averaged over A), the present excitation energy distributions are confirmed in absolute scale.
Finally we mention that TSM-FINESSE has already successfully applied to describe fragment data, neutron multiplicity and neutron emission distributions (energy spectra as well as angular distributions) for a large number of actinides undergoing spontaneous and induced fission (up to $\approx$ 20 MeV neutron incidence energy). TSM-FINESSE reproduces experimental trends without parameter fit.

REFERENCES

1. M. G. Hines et al., Proc. Symp. Nucl. Safeguards and Techn.,10-14 November 1986, Vienna,Austria,Vol.2, p.287
2. J. W. Boldeman, and M. Lammer, Proc. of Conf. "Nuclear Data for Sci. and Techn.", Mito 1988, JAERI-1988, p.937
3. R. L. Walsh, Proc. of Conf. 50 Years with Nuclear Fission, Gaithersburg, U.S.A. 25-28 April 1989, Ed. J. W. Behrens, A. D. Carlson, ANS 1989, Vol.1 p.274
4. D. G. Madland, and J. R. Nix, Nucl. Sci. Eng. 81, 213 (1982)

5. H. Märten et al., Proc. Int. Symp. on Nucl. Phys., Gaussig 1987, GDR, p.148
6. H. Märten, Proc. IAEA AGM on Nuclear Theory for Fast Neutron Nuclear Data Evaluation, Beijing, 12-16 Oct. 1987, IAEA-TECDOC-483 (1988) 148
7. H. Märten, and D. Seeliger, J. Phys. G 14, 211 (1988)
8. K. Arnold et al., Nucl. Phys. A502, 325 (1989)
9. A. Ruben, H. Märten, and D.Seeliger, 'Fission Neutrons' Statistical Emission', Present report, paper No. 1
10. H. Märten, and D. Seeliger, Nucl. Sci. Eng. 93, 370 (1986)
11. A. Ruben, H. Märten, and D. Seeliger, 'Energy Partition in Nuclear Fission', Present report, paper No. 2
12. E. Alleart, Nucl. Phys. A380 (1982), p.61
13. C. Wagemans et al., Nucl. Phys., A502 (1989), p.287
14. P. Schillebeeckxs et al., Proc. 4th Int. Symp. Smolenice (1985), p.375
15. H. Thierens et al., Phys. Rev. C29, 498 (1984)
16. W. W. Malinovski et al., Jad. Konst., 5(54) (1983), p.19
17. U. Brosa et al., Z. Phys. A325, 241 (1986)
18. H. Märten, Proc. Conf on 50th Anniversary of Nuclear Fission, Leningrad, 1989, to be published
19. Z. A. Alexandrova et al., At. Energy 36 (1974), p.282
20. T. W. Bonner, Nucl. Phys. 23 (1961), p.116
21. V. I. Bol'shov et al., Fizika deleniya atomnykh yader (Pysics in Nuclear Fission) Atomizdat (1962), p.127
22. L. M. Belov et al., Sov. Journ. of Nucl. Phys. 9 (1969), p.421

Theoretical model application to the evaluation of fission neutron data up to 20 MeV incidence energy

A. Ruben, H. Märten, and D. Seeliger
Technische Universität Dresden

Abstract: *A complex statistical theory of fission neutron emission combined with a phenomenological fission model has been used to calculate fission neutron data for ^{238}U. Obtained neutron multiplicities and energy spectra as well as average fragment energies for incidence energies from threshold to 20 MeV (including multiple- chance fission) are compared with traditional data representations.*

1. Introduction

Recent requirements of neutron data for nuclear engineering include fission neutron multiplicities and emission spectra in a wide incidence energy range. For the development of fusion-fission-hybrid reactors, the knowledge of the prompt fission neutron spectrum as a main part of the total neutron emission cross section for neutron induced reactions of ^{238}U is of special interest. Present nuclear data applications are based on fission neutron spectra approximated by a simple Maxwellian or Watt distribution with parameters deduced empirically.
In the present work, fission neutron data for ^{238}U are described in the framework of the statistical evaporation model FINESSE /1/ combined with parts of fission theory. Statistical reaction theory including fission channel has been applied to determine partial cross sections for multiple chance fission occurring at incidence energies higher than about 6 MeV. Based on these calculations the average neutron energies which are correlated with the temperatures of an approximative Maxwellian are presented. Changes in the deviation from reference Maxwellians are discussed.

2. The Model

In the sense of consideration of the complexity of nuclear fission to a necessary extend, the present calculations of fission neutron data have been based on fission fragment characteristics relevant within FINESSE. These data, i.e. excitation energy $\overline{E}^*(A)$ and total kinetic energy $\overline{TKE}(A)$, are obtained within a phenomenological scission point model (two-spheroid-model TSM /2/) including semi-empirical, temperature- dependent shell-correction energies. Based on a general energy balance of scission (cf. Terrell /3/) extended by considering pre-scission kinetic energy as well as dissipative energy the nuclear potential depending on fragments deformation is minimired to determine the most probable energy partition. In this way it is possible to deduce average excitation and kinetic energy of the fragments. To describe fragment deformation at scission we use an empirical relation between deformability and shell-correction energy according to Kildir and Aras /4/.
Based on the well known fragment data of $^{252}Cf(sf)$ and $^{235}U(n_{th},f)$ a set of semi-empirical shell-correction energies for zero excitation at scission has been obtained. It provides the basis for any application. In the calculation of the fragment data for $^{238}U+n$ the actual shell-correction energies are deduced by interpolating these parameter sets taking into account the diminution of shell correction energies due to the intrinsic temperature at scission. This washing out of shell effects, depending on the excitation energy of the fissioning nucleus, is considered according to Bohr and Mottelson /5/. Using these shell energies the fragment deformabilities and, consequently, the excitation and kinetic energies are calculated.
Energy balance of fragment de-excitation after scission yields the relationship between the average neutron multiplicity $\overline{\nu}(A)$ and the fragment excitation energy $\overline{E}^*(A)$.
The fragment mass distribution Y(A) is obtained by superposition of 5-Gaussians. This approach is supported by the existence of several fission modes. Each Gaussian is characterized by the average value, the variance and the weight. These parameters depend on the mass and the excitation energy of the fissioning nucleus and have been fitted for the Th-Cf region.
Based on these fragment data the prompt fission neutron spectra are calculated within the model FINESSE. Assuming evaporation of neutrons from fully accelerated fragments as the main emission mechanism the center-of-mass system (CMS) spectrum is calculated by the help of an extended Weisskopf ansatz. Considering cascade emission mechanism as well as the initial distribution in fragment excitation energy a temperature distribution P(T) can be deduced

taking into account the relation between excitation energy and temperature as given by statistical thermodynamics.
The effect of competition between neutron and γ-ray emission on spectral shape approximated within temperature integration by introducing alower temperature limit. This limit as a free parameter has been adjusted on the basis of well-known ^{252}Cf(sf) standard spectrum. Further, spin-dependent CMS-anisotropy is included. Thus, the CMS-spectrum is calculated for each fragment of mass number A. After transformation into the laboratory system (LS) the final spectrum N(E) is calculated by the superposition of fragment spectra weighted by the fragment mass yield.

3. Multiple-Chance fission

At incidence energies higher than about 6 MeV multiple-chance fission has to be taken into account, i.e. (n, xnf), where x denotes the number of pre- fission neutrons for a given chance. Note that fission fragment characteristics as well as fission neutron spectra in the case of multiple chance fission have to be calculated for all chances energetically possible.This has to be considered in the model application by separate calculation for each chance and a following summation weighted by the partial fission cross sections.
Starting with the calculation of fragment data for all chances within TSM taking into account the changes in mass and excitation energy of the compound nucleus after emission of pre-fission neutrons, FINESSE is applied to deduce the neutron data.
As discussed above, the total value of neutron multiplicity and total kinetic energy are given by a superposition weighted by the partial fission cross section $\sigma_{f,x}$ for chance x,

$$\bar{\nu}_{tot} = \frac{1}{\sigma_{f,tot}} \sum_{x=0}^{x_{max}} \sigma_{f,x} \, (\bar{\nu}_x + x) \qquad (1)$$

(including pre-fission neutrons)

$$\overline{TKE}_{tot} = \frac{1}{\sigma_{f,tot}} \sum_{x=0}^{x_{max}} \sigma_{f,x} \, \overline{TKE}_x \qquad (2)$$

with

$$\sigma_{f,tot} = \sum_{x=0}^{x_{max}} \sigma_{f,x} \qquad (3)$$

The partial fission cross sections as shown in Fig.1 are calculated by the code STAPRE (Maslow-version Minsk /6/).

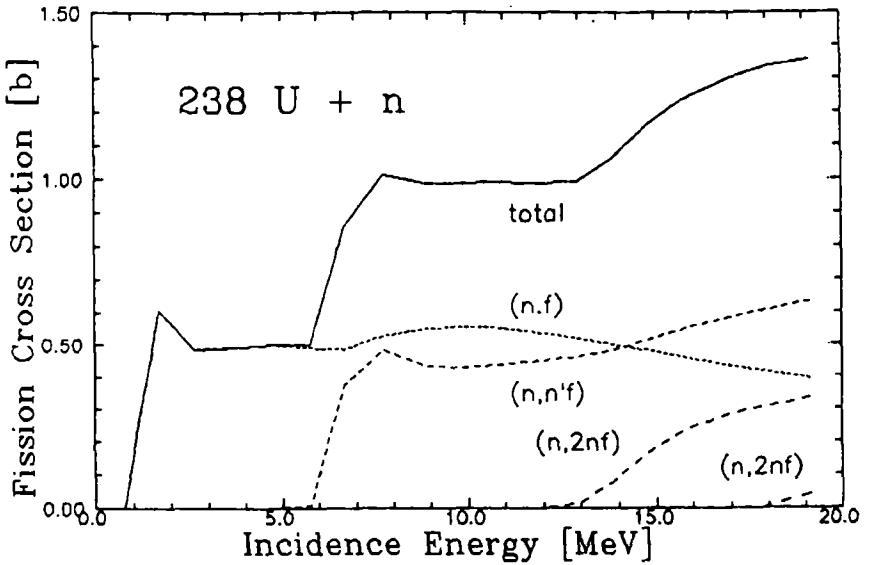

Fig.1 Total and partial fission cross section for the neutron induced fission of ^{238}U (STAPRE)

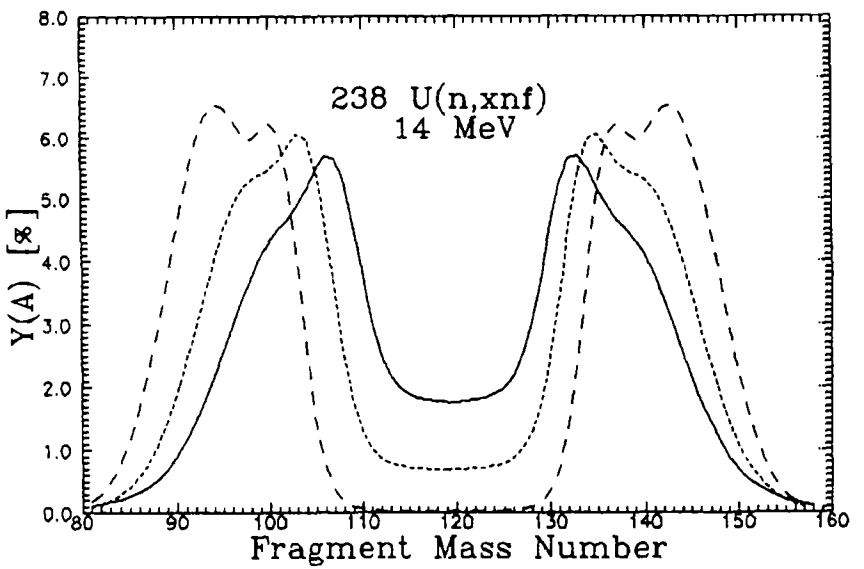

Fig.2 Fragment mass yield for ^{238}U+n at 14 MeV incidence energy. The continous, dotted, and dashed curres correspond to first-, second-, and third-chance fission, respectively.

Within a 5-Gaussian approach to the the fragment mass yield, changes of the compound nucleus and its excitation energy are considered, too. The distribution parameters are determined by the excitation of the fissioning nucleus above its fission barrier. As an example, Fig.2 shows the mass yield curves for the three chances at 14 MeV incidence energy.

Finally, the prompt fission neutron spectrum is calculated within FINESSE for each chance using the corresponding fragment data.

As shown in the case of fragment characteristics, the total spectrum is given by

$$N(E)_{tot} = \frac{1}{\sigma_{f,tot}} \sum_{x=0}^{x_{max}} \sigma_{f,x} \, N(E)_x \qquad (4)$$

(Here, $N(E)_x$ is normalized to $\bar{\nu}_x$.)

The total average energy of post-fission neutrons can be calculated on the basis of the total spectrum (eq.(4)) or using

$$\bar{E}_{tot} = \frac{\sum \sigma_{f,x} \, \bar{\nu}_x \, \bar{E}_x}{\sum \sigma_{f,x} \, \bar{\nu}_x} \quad (x=0,1,2) \qquad (5)$$

4. Results

In Fig. 3, the total neutron multiplicity (averaged over all fragments) is plotted versus incidence energy. Calculated values are in good agreement with measured data in the whole incidence energy range considered.

The comparison of calculated total kinetic energies with experimental data is more difficult, since measured data exist only up to 6 MeV incidence energy. Further, this quantity is very sensitive to the fragment mass distribution involved. As depicted in Fig. 4, the striking trend in the TKE behaviour, i.e. the decrease with incidence energy, is well reproduced. Above the threshold for second- chance fission, the decrease is suppressed by higher TKE values for the (n, n´f) reaction a.s.o.!

Fig. 5 shows the average LS-neutron energy asfunction of the incidence energy.Corresponding values deduced from Terrell relation /3/, i.e.

$$\bar{E}\,(\bar{\nu}) = 0.75 + 0.65 \sqrt{\bar{\nu} + 1} \quad , \qquad (6)$$

are also included. Obviously, this empirical relation doesn´t account for effects of higher order fission chances on $\bar{E}$.

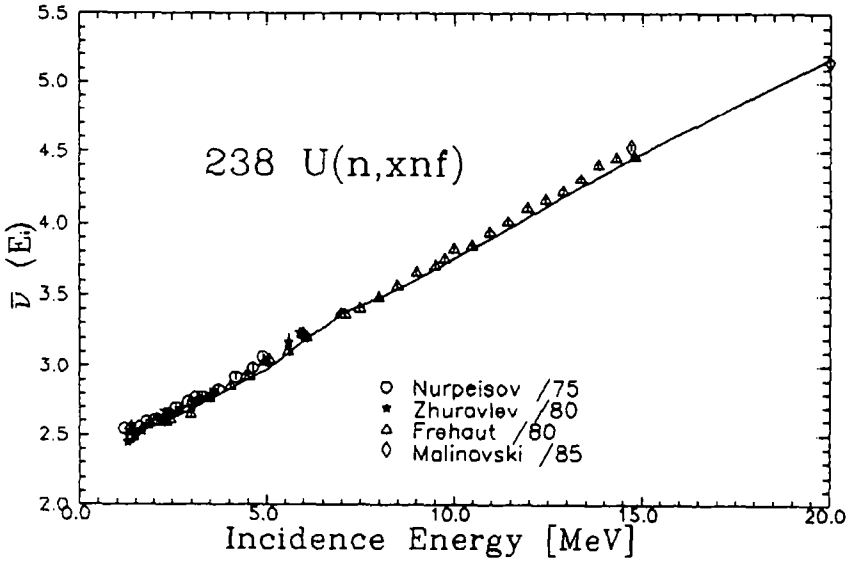

Fig. 3 Total neutron multiplicity as function of incidence energy compared with experimental data /7-10/ for the neutron induced fission of ^{238}U

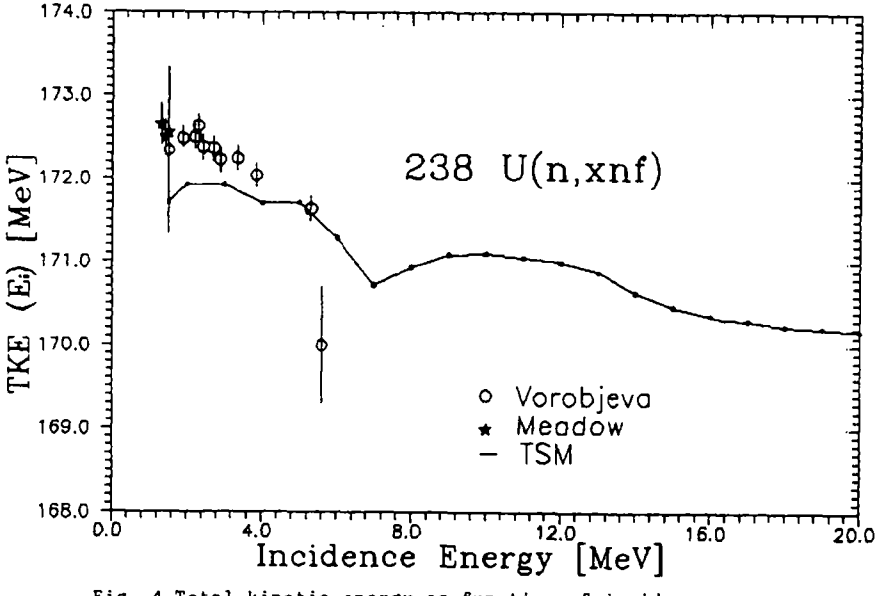

Fig. 4 Total kinetic energy as function of incidence energy compared with experimental data /11,12/for th neutron induced fission of ^{238}U

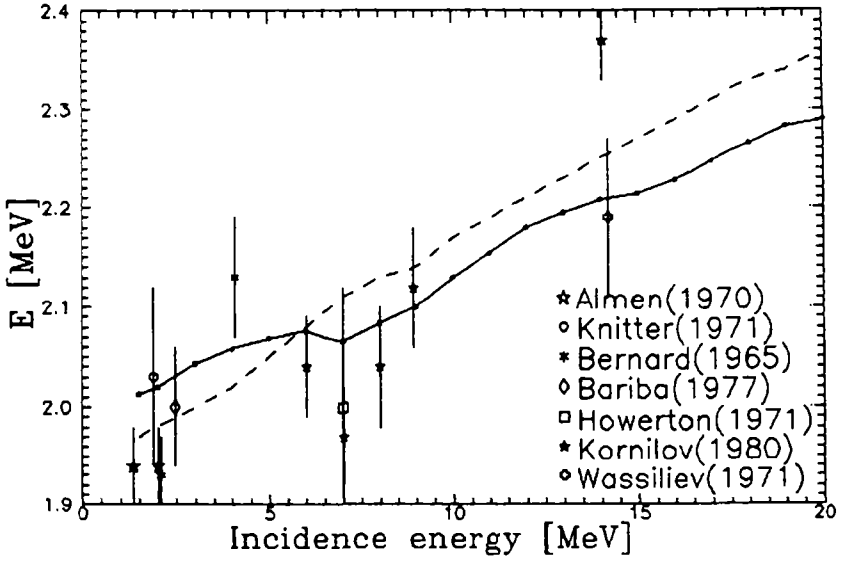

Fig. 5 Average LS-neutron energy as function of incidence energy (solid line -FINESSE, dashed line - Terrell's relation, experimental data - ref./13-19/)

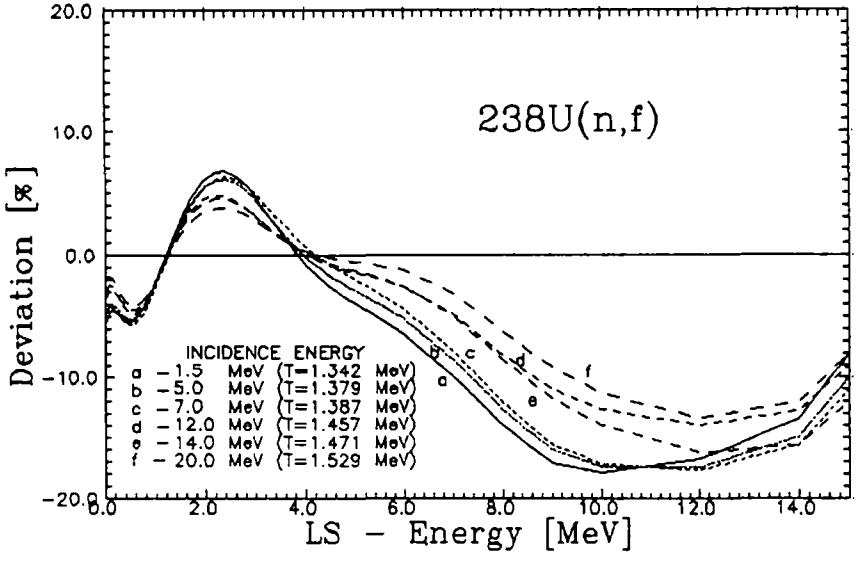

Fig. 6 Deviation of calculated fission neutron spectra from Maxwellian for different incidence energies for multiple chance fission of ^{238}U

Again, calculated and measured data are in good agreement within experimental uncertainties. Note that the calculated average energies correspond to the post-fission neutrons only. That cause differences to experimental data including pre-fission neutrons at E >6 MeV, too. Further, the average energy of a measured spectrum is very sensitive to the neutron energy range taken into account. The calculated energies are relevant to the entire spectrum.
In a first order approximation, the prompt fission neutron spectrum can be described by a Maxwellian, whose temperature is deduced from the average neutron energy ($T=2/3\bar{E}$). The systematic calculations performed in this work show that the deviation from this distribution are similar for all incidence energies considered.In Fig. 6, this is represented for 6 incidence energies.

5. Conclusions

The theoretical description of fission energetics and neutron emission within the model-complex TSM and FINESSE reproduces general trends in fragment characteristics and in prompt fission neutron spectra in the whole incidence energy region up to 20 MeV. Especially, the total neutron multiplicities are in a good agreement with measured data. The calculation of fission neutron spectra has shown that a first order approximation by a Maxwellian distribution is possible. However, an application of the empirical relation between average energy and average neutron multiplicity involves uncertainties, especially in the case of multiple chance fission.

References

1. A. Ruben, H. Märten, and D.Seeliger, 'Fission Neutrons' Statistical Emission', Present report, paper No. 1
2. A. Ruben, H. Märten, and D. Seeliger, 'Energy Partition in Nuclear Fission', Present report, paper No. 2
3. J. Terrell, Proc. IAEA Symp. on Phys. and Chem. of Fission, Salzburg, 1965 (Vienna, 1965) Vol. II, p. 3
4. M. Kildir and N.K. Aras, Phys. Rev. C25, 365 (1982)
5. A. Bohr and B.R. Mottelson, "Nuclear Structure" (Benjamin, New York, 1975), vol. II
6. A. V. Ignatjuk, V. M. Maslov, and A. B. Paschenko, Sov. J. Nucl. Phys. 47(2) (1988), p.224

7. B. Nurpeisov et al., At. Energ. 39 (1975), p.199
8. W. V. Zhuravlov et al., "Investigation of the interactions of neutrons with ^{298}nuclei", INDC(CCP) - 154/L, Vienna 1980
9. J. Frehaut et. al., "Recent results on nue-prompt measurements between 1.5 and 15 MeV", Paris 1980
10. W. W. Malinovski et al., Proc. of Int.Conf. Santa Fe, 13.-17. May 1985
11. V. G. Vorob'eva et al., Yad. Konst. 15 (1974), p.3
12. J. W. Meadows, Phys. Rev. 177 (1969), p.1817
13. E. Almen et al., "Nuclear data for reactors", Helsinki 1970, p.93
14. H. - H. Knitter, Z. Phys. 244 (1971), p.345
15. E. Barnard et al., Nucl. Phys. 71 (1965), p. 228
16. Bariba et al., At. Energ. 43 (1977), p.266
17. R. J. Howerton and R. Dayas, Nucl. Sci. and Eng. 46 (1971), p.414
18. K. W. Kornilov et al., Kiev 1980, Vol. 3, p.104
19. J. A. Wassiliev, JETP 38 (1960), p.671